T.R.
VAN YUZUNCU YIL UNIVERSITY
INSTITUTE OF NATURAL AND APPLIED SCIENCES
DEPARTMENT OF PHYSICS

THE INVESTIGATION OF THE EFFECT OF METAL TYPE ON THE ELECTRICAL PROPERTIES OF HYBRID STRUCTURE BASED ON FUNCTIONAL DYE

M. Sc. THESIS

PREPARED BY: Sabiha Abdullah OMARBLI
SUPERVISOR: Assoc. Prof. Dr. Arife GENÇER İMER

VAN-2020

T.R.
VAN YUZUNCU YIL UNIVERSITY
INSTITUTE OF NATURAL AND APPLIED SCIENCES
DEPARTMENT OF PHYSICS

THE INVESTIGATION OF THE EFFECT OF METAL TYPE ON THE ELECTRICAL PROPERTIES OF HYBRID STRUCTURE BASED ON FUNCTIONAL DYE

M. Sc. THESIS

PREPARED BY: Sabiha Abdullah OMARBLI

VAN-2020

ACCEPTANCE and APPROVAL PAGE

This thesis entitled "**The Investigation of The Effect of Metal Type on The Electrical Properties of Hybrid Structure Based on Functional Dye**" presented by Sabiha Abdullah OMARBLI under supervision of Assoc. Prof. Dr. Arife GENÇER İMER in the department of Physics has been accepted as a M. Sc. thesis according to Legislations of Graduate Higher Education on 14/01/2020 with unanimity / majority of votes members of jury.

Chair: Assoc. Prof. Dr. Murat AYCİBİN   Signature:

Member: Assoc. Prof. Dr. Arife GENÇER İMER   Signature:

Member: Assist. Prof. Dr. Hasan AĞIL   Signature:

This thesis has been approved by the committee of The Institute of Natural and Applied Science on ..../.........../.......... with decision number ....

Signature:
....
Director of Institute
Prof. .... ENSOY
Enstitü Müdürü

THESIS STATEMENT

All information presented in the thesis obtained in the frame of ethical behavior and academic rules. In addition all kinds of information that does not belong to me have been cited appropriately in the thesis prepared by the thesis writing rules.

Signature

Sabiha Abdullah OMARBLI

ABSTRACT

THE INVESTIGATION OF THE EFFECT OF METAL TYPE ON THE ELECTRICAL PROPERTIES OF HYBRID STRUCTURE BASED ON FUNCTIONAL DYE

OMARBLI, Sabiha Abdullah
M. Sc. Thesis, Department of Physics
Supervisor: Assoc. Prof. Dr. Arife GENÇER İMER
January, 2020, 81 Pages

In this thesis, the effect of phenol red an organic interlayer in a metal semiconductor diode with different metal top contact was studied using various methods. The performance of the diodes was evaluated by examining the current-voltage (I-V) and capacitance-voltage (C-V) measurements at room temperature using thermionic emission, Norde and Cheung-Cheung methods in calculation. The electrical parameters such as barrier height Φ_b, ideality factor n, and series resistance R_s were determined using the I-V measurements of the diodes. The effect of metal type (M=Ag, Cu, Ni, Pd, Sn) on the electronic parameters has been investigated and compared with each other. The obtained results show that all the devices with and without the organic interlayer have rectification behavior. The barrier height values of the devices increases with inserting the organic layer. The highest value of barrier height was 0.738 eV with the Sn metal and the lowest value was 0.600 eV with Ni metal were obtained by I-V measurements.

C-V measurements were used to obtain electrical parameters of fabricated devices. This measurement showed that the organic thin film has been enhanced the electrical properties of the diodes, and these results were agreement with the results obtained from other methods. The obtained results showed that the electrical properties of devices are strongly dependent on the metal type, and presence of interfacial layer. Thus, the modification of these parameters, and increment of the device performance are possible, by using appropriate metal and the organic interfacial layer.

Keywords: Electrical properties, Fenol red, Metal work function, Organic interfaces.

ÖZET

ORGANİK BOYA TABANLI HİBRİT YAPININ ELEKTRİKSEL PARAMETRELERİNE METALİN İŞ FONKSİYONUNUN ETKİSİNİN İNCELENMESİ

OMARBLI, Sabiha Abdullah
Yüksek Lisans Tezi, Fizik Anabilim Dalı
Tez Danışmanı: Doç. Dr. Arife GENÇER İMER
Ocak, 2020, 81 Sayfa

Bu çalışmada, farklı iş fonksiyonuna sahip beş ayrı metal ile organik bileşenli metal-yarıiletken aygıtlar üretildi. Metal ile yarıiletken arasına kaplanan fonksiyonel organik boyar fenol kırmızısı arayüzey tabakasının aygıt performansına etkisi incelendi.

Üretilen aygıtların performansı akım-gerilim ve kapasitans-gerilim grafiklerinden elde edilen verilerin termiyonik emisyon, Norde ve Cheung denklemlerinde kullanılması ile incelendi. Diyotların elektriksel ölçümlerine dayanarak, bariyer yüksekliği, idealite faktörü n ve seri direnç gibi parametreler hesaplandı. Metal tipinin (M = Ag, Cu, Ni, Pd, Sn) elektronik parametreler üzerindeki etkisi incelenip ve birbirleri ile karşılaştırıldı. Elde edilen sonuçlar, organik arayüzey içeren tüm aygıtların doğrultucu özelliğe sahip olduğunu gösterdi. Organik tabakanın yerleştirilmesiyle aygıtların engel yüksekliği değerleri artmıştır. En büyük engel yüksekliği değeri Sn metali ile (0.738 eV), en düşük engel yüksekliği değeri Ni metali ile (0.600 eV) elde edildi.

Üretilen diyotların elektronik parametreleri C-V ölçümleri ile hesaplandı. Organik ince film katmanın diyotların elektriksel özelliklerini iyileştirdiği tespit edildi. C-V'den elde edilen sonuçlar diğer yöntemlerden elde edilen sonuçları doğruladı. Elde edilen bulgular, aygıtın elektriksel özelliklerinin metal tipine ve arayüzey varlığına bağımlı olduğunu gösterdi. Arayüzey yardımıyla bu değerleri ayarlamanın ve aygıt performansını iyileştirmenin mümkün olduğu rapor edildi.

Anahtar kelimeler: Elektriksel özellikler, Fenol kırmızısı, Metal iş fonksiyonu, Organik arayüzey.

ACKNOWLEDGMENT

TABLE OF CONTENTS

LIST OF TABLES

LIST OF FIGURES

SYMBOLS AND ABBREVIATIONS

Some symbols and abbreviations used in this study are presented below, along with Descriptions.

Abrivation	Description
ΔE_a	Activation energy for charge carriers
Ag	Silver
Al	Aluminum
C-f	Capacitance dependent frequency
Cu	Copper
C-V	Capacitance-voltage characteristics
GaAr	Galium arsenide
HF	Fluoric acid
HOMO	Highest occupied molecular orbital
InGa	Indium-gallium
InP	Indium phosphide
I-V	Current-voltage characteristics
LCAO	Linear combination of atomic orbitals
LUMO	Lowest unoccupied molecular orbital
MIS	Metal-Insulator-Semiconductor
MS	Metal-Semiconductor
NC	Negative capacitance
Ni	Nickel
OFET	Organic field-effect transistor
OLED	Organic light emitting diode
Pd	Palladium
PSP	Phenolsulfonphthalein = PSP
Sn	Tin
SnO_2	Tin dioxide (stannic oxide)

Symbols	Description
A	Area
π^*	Anti pi bond
μ	Mobility of charge carriers
μ_0	Zero-field mobility
A*	Effective Richardson constant
E	Electrical field
Ec	Conduction band energy
E_F	Fermi energy level
E_{FM}	Metal Fermi level
E_{Fsc}	Semiconductor Fermi level
E_g	Band gap energy
ε_r	Relative permittivity of the semiconductor
Ev	Valence band energy
ε_o	Permittivity of vacuum
I_o	Saturation current
k_B	Boltzman constant
m_e	Effective mass
p	P orbital
s	S orbital
σ	Conductivity
σ_o	Intrinsic conductivity of charge carriers
Φ_{bn}	Barrier height of n-type semiconductor
Φ_{bp}	Barrier height of p-type semiconductor
$\hbar$	Plank constant
Φ_b	Barrier height
Φ_m	Work function
Φ_s	Semiconductor work function
π	Pi bond

n	Ideality factor
$\mathbf{N_a}$	Density of acceptors
$\mathbf{N_d}$	Density of donors
$\mathbf{N_{ss}}$	Density distribution of interface states
$\mathbf{N_v}$	Denisity of state in valence bond
$\mathbf{^oC}$	Celiseus temperature
q	Electron charge
R	Rectification ratio
$\mathbf{R_C}$	Contact resistance
$\mathbf{R}_s$	Series resistance
T	Absolute temperature
UV	Ultra viole light
V	Voltage
$\mathbf{V_0}$	Voltage at zero bias
$\mathbf{V_{bi}}$	Built in potential
$\mathbf{V_i}$	Applied voltage
W	Depletion width
$\boldsymbol{\chi}$	Electron affinity
$\boldsymbol{\sigma}$	Sigma bond
$\boldsymbol{\sigma} *$	Anti Sigma bond

1. INTRODUCTION

Organic materials with attractive electronic and optoelectronic properties are in high demand for functional electro-optical device applications. Research on synthetic polymer and organic small molecules has gained a great deal of attention due to their potential applications such as low cost, ultra-thin, and flexible products, and it is expected to have a revolutionary role in modern day life.

Organic electronics are rapidly evolving field with enormous number of applications having high possibility for commercial profits. Electronic devices based on organic materials can be fabricated by simple processing techniques for the investigation in academic and industrial laboratories, because of the ability to mass production of flexible devices. organic semiconductor materials are favored, because they allow for a low cost of device fabrication and the use of flexible substrates. Organic devices also possess transparent advantages and light weight compared to silicon-based devices. These organic compounds are being developed for improved resistance to thermal and environmental stresses, which is one of the major challenges in the field, encompassing interdisciplinary research areas. These devices are good candidate for next generation electronics with energy-efficient security systems, sensors, photonics, and spintronic memories.

Organic electronic devices still need further optimization to fulfill the requirements for successful commercialization. For many applications, available organic materials do not provide satisfactory performance and stability, which hinders the possibility of a large-scale production. Therefore, the key ingredient needed for a successful improvement in stability and performance of organic electronic devices is in-depth knowledge of physical and chemical properties of molecular and polymeric materials. Since many applications consist of several thin film layers made of inorganics, and organic materials, the understanding of both organic and organic hybrid interfaces is still another important issue, necessary for the successful development of organic electronics devices.

In this thesis, the role of interfacial layer of an organic dye, which is inserted in a metal-semiconductor diode with different top contact metal work function are studied in order to investigate the effect of the organic interfacial layer on the performance and electrical properties of the diodes. The treatment is performed using spin coater for inserting the solution of the organic dye, and thermal evaporator method was used for forming back contact, also front contact electrodes. Several calculation methods like *I-V*, *C-V*, Norde's and Cheung-Cheung's functions are used to verify and prove the results, which show the performance and the electrical properties of the diodes.

2. LITERATURE REVIEW

Walter Schottky, (1886-1976), a German physicist discovered an irregularity in emission of thermions in vacuum tube, now known as *Schottky effect* in 1914. He was one of the first to point out the existence of "electron and holes" in the valence band structure of semiconductors. In 1938, he developed a theory that explained the rectifying behavior of metal-semiconductor contact as dependent barrier layer at the surface of contact between the two materials. The metal semiconductor diodes later built on the basis of this theory and it is called Schottky barrier diodes (Sze and Ng, 2006).

The discovery of electrical conductivity in organic materials, is resulted in a wide field for researching in a material science that previously was thought to be insulating materials, in this field. Organic Schottky barrier diodes are imperative for a wide range of electronic and optoelectronic industry applications used in the devices. Its properties make it be used in many applications including organic photovoltaic devices, organic light-emitting diodes (OLEDs), organic field effect transistors (OFETs), organic solar cells and etc….

In recent years, organic semiconductors showed great development to use as a commercial alternative to traditional inorganic materials. In 1977, the first highly conducting polymer chemically doped polyacetylene was discovered, which improved that polymer could be used as electrically active materials, this result leads to huge research efforts on conjugated organic materials, and in 2000, the noble prize in chemistry was awarded to Alan J. Heeger, Alan G. McDiarmid and Hideki Shirakawa for "The discovery and development of conductive polymers (Stella, 2009).

Therefore, the key ingredient needed for a successful improvement in performance and stability of organic electronic devices is in depth knowledge of physical and chemical properties of molecular and polymeric materials. Since many applications encompass several thin film layers made of organics, and often also inorganic materials, the understanding of both organic inorganic hybrid interfaces is yet another important issue necessary for the successful development of organic electronics.

(Chankaya and Uchar, 2004) fabricated metal/p-Si schottky diodes with different metals (Mn, Cd, Al, Bi, Pb, Sn, Sb, Fe and Ni) as top contacts, by using thermal evaporation method. They reported that the Schottky barrier diodes weakly depend on the work function of the contact metal and the Fermi level is pinned at about 0.661eV below the condition band. The value of ideality factor which they calculated using *I-V* measurements was in the range of 1.057 to 1.831 and the values of barrier height were in the range of 0.567 eV to 0.854 eV.

Yakuphanoglu and Senkal, 2007) investigated the electrical properties of Al/PANE/Si diodes with Polyaniline as an organic interlayer. They calculated the ideality factor and barrier height of the diodes by using *I-V* and *C-V* measurements, the values that they found was 2.89 and 0.85 eV for ideality factor and barrier height respectively

(Aydin and Yakuphanoglu, 2007) prepared Al/FSS/p-Si diode with fluorescein sodium salt as an organic interlayer. They used *I-V* measurements to investigate the electrical properties of Ag/FSS/p-Si diode. They reported that the diode showed rectifying behavior and indicated a non-ideal *I-V* behavior with an ideality factor higher than the unity. Also the ideality factor decrease with increase of temperature and barrier height increases with increasing of temperature, the barrier height value of the diode was 0.92 eV and 0.75 eV from *C-V* and *I-V* measurements respectively.

Zubair Ahmad et al. (2008) fabricated and studied the electrical properties of Au/methyl-red/Ag surface type Schottky diode. They used *I-V* measurements to calculate barrier height and ideality factor of diodes, and they reported that the diode showed good rectifying behavior.The values of barrier height were 0.254 eV and 1.93 for ideality factor by using *I-V* characteristics and by using cheungI and CheungII calculation, they found 0.26 eV for barrier height and 1.89 for ideality factor meanwhile the series resistance were calculated was 1.1kΩ.

Yakuphaoglu (2008) investigated the electrical properties of Al/p-Si/DB6MEH diode. He used *I-V* and *C-V* measurements to calculate the ideality factor, barrier height and series resistance through *I-V* and Cheung-Cheung methods. The value of ideality factor was 1.92 and the value of barrier height was 0.93 eV and 0.75 eV from *C-V* and

I-V measurements, respectively. The value of series resistance was 19.55 kΩ and 20.44 kΩ from d*V*/dln*I* vs *I* and H (*I*) vs *I* plots, respectively.

Yakuphaoglu et al. (2008) investigated the electrical properties of Al/p-type silicon phthalocyaninato cobalt (ll) organic diode by *I-V* and *C-V* characteristics. They calculated the electrical parameters such as ideality factor, barrier height and series resistance of Al/p-Si/CoPc contacts, and the values were 1.33 for ideality factor and 0.90 eV for barrier height which was higher than the barrier height value of Al/p-Si Schottky diode, the value of series resistance was 314.5 kΩ.

(Gullu and Turut, 2009) used (phenolsulfonphthalein=PSP) as an organic interlayer in fabricating Al/p-Si diode. In their work, they used *I-V* characteristics to calculate the ideality factor *n* and barrier height Φ_b for the diodes with and without (PSP) organic interlayer. The values of ideality factor and barrier height were 1.45 and 0.81 eV for Al/PSP/p-Si diode, respectively, and the value of barrier height for Al/p-Si was 0.50 eV. They also calculated the interface-state density of the MIS diode which is varied from 3.00×10^{13} to 2.99×10^{12} eV^{-1} cm^{-2}.

Gullu et al. (2009) prepared Al/p-Si Schottky diodes with and without organic Congo Red (CR) interlayer. They used spin coating method to form an organic thin film of (CR) on p-Si semiconductor wafer. By using *I-V* characteristics, they calculated the ideality factor and the barrier height of the diodes which were 1.68 and 0.77 eV, respectively for organic interlayer diodes. They reported that the barrier height value of the diodes with organic interlayer is greater than the value of the diodes without organic interlayer which is 0.50 eV, and the MIS devices showed a good rectifying behavior and the (CR) organic interlayer increased the effective barrier height value by influencing the space charge region of Si.

Kim et al. (2010) fabricated organic Schottky diodes by printing process. The organic material was P3HT with different thickness 30 nm and 100 nm. The electric characteristic of the diodes was with an input voltage of 20 $_{p-p}$, the output characteristics showed DC 5.3 V at 100Hz and DC 3.2 V at 1MHz. They reported that the output voltage decreased more drastically in the thicker diode than the thinnest diode when the frequency is increased.

Verma et al. (2010) studied the relation between work function of two different top contact metals of Schottky diodes and barrier height value of them. They fabricated Schottky diodes by depositing 100 nm thickness of gold and platinum metals on n-type Si wafer by using e-beam evaporation method. The *I-V* characteristics showed that the barrier height of the diodes depends linearly on the work function of the metals, and there is very weak dependence of Schottky barrier height on metal work function, the ideality factor was found as 1.33 and 1.58 for gold and platinum, respectively.

(Gullu and Turut, 2010) prepared Al/OG/p-Si MIS diodes with and without (Orange G=OG) organic dye as an interfacial layer by spin coating method they deposited thin film on p-Si semiconductor. They reported that the MIS has a good rectifying behavior. By using *I-V* measurements they calculated the ideality factor and barrier height of the Al/OG/p-Si diode, and the values were 1.73 and 0.77 eV for ideality factor and barrier height, respectively. Where the value of barrier height was 0.50 eV for diode without organic OG interlayer.

Gullu et al. (2012) fabricated Cu/n-InP Schottky junction with organic dye (PSP) Phenol red by using solution cast process. They used *I-V* measurements to measure the barrier height value of the diode which was 0.82 eV, and by using *C*-V measurement the diffusion potential and the barrier height have been calculated 0.73V and 0.86 eV, respectively.

Karadeniz et al. (2013) prepared Al/p-Si diodes with and without rubrene layer deposited by using spin coating method. By analyzing the I-V and *C-V* measurements at room temperature they calculated the basic parameters such as ideality factor, barrier height and series resistance of the diodes with and without rubrene interlayer. The values of ideality factor were 1.51 and 1.22 calculated from I-V measurements for Al/p-Si with and without rubrene interlayer, respectively. The estimated barrier height was found to be 0.649 eV and 0.771 eV for the diodes with and without rubrene layer, respectively. The value of barrier height calculated from *C-V* data for Al/p-Si with rubrene layer was 0.820 eV, which is higher than the value from *I-V* measurements.

Yuksel et al. (2013) prepared Au/PMI/p-Si Schottky barrier diodes with perylene mono imide (PMI) organic interlayer. They calculated the electrical parameters such as ideality factor, barrier height and series resistance of the diodes by using *I-V*

characteristics by *I*-V and Cheung-Cheung methods for calculation and the values of ideality factor, barrier height and series resistance of diode at room temperature was found to be as 3.53, 0.567 eV and 188.2 Ω, respectively.

Yıldıs et al. (2013) fabricated ITO/PEDOT:PSS/Poly ((9,9-dioctylfluorene)-2,7-diyl(2-dodecyl-benzo[1,2,3]-triazolle))(PFTBT)/Au devices. They used *I-V* and *C-V* measurements to calculate the electrical parameters such as ideality factor, barrier height and series resistance of the diode by using Norde and Cheungs methods. The values of ideality factor, barrier height and series resistance was 3.8, 0.711 eV and 19.267 kΩ, respectively.

Taşçıoglu et al. (2013) investigated the effect of metal work function on the formation of barrier height at metal-semiconductor MS interface. They prepared CdS/SnO$_2$/In-Ga structures with different metal contacts Al, Ag, Te and Au. By using *I-V* characteristics at room temperature they calculate the main electrical parameters such as ideality factor n, reverse-saturation current I_s, Zero-bias barrier height Φ_b, series resistance R_s and shunt resistance R_{Sh}. They reported that the barrier height weakly depends on the choice of the metal work function, the values of barrier height of each metal was 0.489 eV, 0.490 eV, 0.583 eV and 0.591 eV for metal contacts Al, Ag, Te, and Au, respectively.

Al Oariny (2014) fabricated Al/p-FSS Schottky diode with Fluorescein Sodium salt as an organic interlayer. He analyzed the *I-V* and *C-V* measurements to calculate the electronic parameters such as barrier height, ideality factor and series resistance of the diode. The values were 0.305, 0.72 eV, 7.73 kΩ for ideality factor, barrier height and series resistance, respectively.

Hyung-JoongYun et al. (2015) prepared Al/p-Si diodes with pristine and 5wt% sorbitol-doped organic PEDOT: PSS interlayer. They reported that the value of barrier height for the diodes with pristine and sorbitol-doped PEDOT: PSS was higher compared to the value of barrier height of conventional Al/p-Si, because of the modification of the effective of barrier height by the organic interlayer.

Kirsoy et al. (2015) fabricated Au/P3HT/n-GaAr Schottky diode. They investigated the electrical properties of the diodes at room temperature. By using current–voltage method they determined the electrical properties. The value of ideality

factor was found as 2.45 and barrier height value was 0.85 eV. They concluded that the diode exhibits non-ideal current–voltage behavior, and the electrical parameter of the diode is higher than the Au/n-GaAr schottky diodes, and it shows rectifying behavior.

Al-Ta'ii et al. (2015) fabricated Al/DNA/p-Si/Al Schottky diode by using deoxyribonucleic acid (DNA) as organic interlayer. By using *I-V* measurements and Cheung-Cheung and Norde methods to calculate ideality factor and barrier height for Al/p-Si/Al with and without DNA interlayer. They demonstrated the effect of alpha irradiation on Al/DNA/p-Si Schottky diodes by investigating its current-voltage characteristics, the diodes exposed for different periods (0-20 min) of irradiation. They reported that the value of ideality factor was varied between 9.97 and 9.57 and barrier height value increases dramatically after 24hr of exposure, this increase is due to the DNA oligonucleotides ability to resist the alpha radiation.

Gullu and Turut, (2015) prepared Cu/DNA/n-InP MIS Schottky diodes. They prepared Cu/n-InP with and without DNA organic interlayer by evaporating in vacum method. By using *I-V* characteristics they determined the ideality factor value as 1.08 and the barrier height value of the diodes with DNA interlayer 0.7 eV and 0.48 eV without DNA interlayer, the diodes showed a good rectifying behavior.

Gullu (2016) prepared Ag/MV/p-InP semiconductor diodes with and without Methyl Violet organic interlayer. He used *I-V* and *C-V* characteristics to calculate the electrical parameters such as ideality factor and barrier height for the diodes. The value of ideality factor was 1.21 and the value of barrier height was 0.84 eV and 0.64 eV for Ag/p-InP with and without (MV) organic interlayer respectively. He reported that the organic interlayer increased the effective barrier height by influencing the space charge region of inorganic semiconductors.

Sekhar Reddy et al. (2016) investigated the electrical properties of Ti/p-type InP Schottky diodes with and without polyaniline (PANI) interlayer. Norde and Cheung calculation methods were used to calculate ideality factor and barrier height by using *I-V* and *C-V* measurements. The values that founded for ideality factor was 1.72, 1.42 for Ti/p-type InP diodes with and without PANI interlayer respectively and the barrier height values was 0.83 eV, 0.66 eV for the diodes with and without PANI interlayer, respectively.

Basman et al. (2016) prepared Ag/POEMO/p-Si Schottky diodes with [4-(prop-2-yn-1-yloxy) phenyl] ethanone-O-methacryloyloxime (POEMO) as organic interlayer. They used I-V characteristics to calculate the electrical parameters such as ideality factor, barrier height and series resistance by IV, Cheung and Cheung methods. The values of ideality factor, barrier height and series resistance were 2.81, 0.70 eV and 2.24 kΩ, respectively. They reported that the value of barrier height of Ag/p-Si with organic interlayer is larger than the value of barrier height without organic layer which was 0.64 eV.

Sekhar et al. (2016) fabricated Ti/p-type InP Schottky diode by using polyaniline (PANI) as organic interlayer and without it. Evaporation method was used to deposit 20nm thickness of PANI and 40 nm thickness of Ti. *I-V* and *C-V* measurement were used to determine electrical parameters at room temperature. The results of barrier height of Ti/p-type InP Schottky diodes with and without PANI interlayer were 0.8 and 0.64 eV, respectively. The value of ideality factor with and without PANI was 1.72 and 1.49, respectively. Both devices showed hight leakage current in the reverse bias region resulted poor rectification behavior. Series resistance that they founded with and without PANI was 14 kΩ and 37 kΩ, respectively. They compared between the two diodes, and barrier height in Schottky diode with PANI interlayer was higher than without PANI interlayer. The inserting of the PANI interlayer leads to the reduction of the interface state density in the Ti/p-type InP Schottky diode.

Imer et al. (2016) fabricated organic-inorganic heterojunction by inserting an interlayer with three different thicknesses on the p-Si substrate. By spin coating method, the DMY thin film with different thickness was deposited on to the p-Si. Using *I-V* measurement at room temperature to investigate the electrical and photoelectrical properties of the devices was analyzed as a function of incident light intensity via solar simulator. *C-V* and *G-V* data were also used to calculate the electrical and photoelectrical properties. Thy reported that the Φ_b value of all heterojunction is higher than energy barrier of traditional Al/p-Si Schottky diodes and the ideality factor of all the devices was greater than one. The devices have strong response to the incident light intensity, and the fundamental electrical parameter can be controlled with the thickness of the interfacial layer at the MS interface.

Mohamad et al. (2017) prepared a metal-organic–metal (MOM) type Schottky diode based on poly (triarlamine) (PTAA) thin film. The (PTAA) thin film was deposited on ITO by spin coating method about 100 nm thicknesses then about 150 nm thickness of Al metal was deposited on the thin film by sputtering technique. They measured frequency dependent conductance *G-f* and capacitance *C-f*, the frequency range varies (12 Hz-100 kHz), and various bias voltage from (0.2-5.0)V with an oscillating wave at room temperature. They reported on the frequency dependent characteristics of the Schottky diode that both capacitance and conductance are sensitive with frequency and bias voltage in which conductance increases as the frequency increases.

Moreover the capacitance is dependent on the frequency up to certain value of it 100 Hz after that decreases at high value of frequency (1-10 KHz). The interface density in Schottky diode determined by *G-V* and *C-V* characteristics are almost constant about $2.8 \times 10^{12} \, eV^{-1}.cm^{-2}$, and it slightly decrease by increasing frequency.

Shkir et al. (2017) used phenol red organic dye to fabricate thin films with different thicknesses as 50, 84 and 91 nm. They studied the optical characteristics of the deposited thin films, UV-Vis-NIR absorbance, transmittance and reflectance spectra measurement were recorded. They reported that thin films showed amorphous nature in X-ray diffraction analysis, and the values of energy gap, refractive index, and dielectric constant vary with thickness of the thin film. The nonlinear optical constant such as: χ^1, χ^3 and n_2 are changed with the thickness of the films, which are in the range of 0.3-1.8, 0.0089×10^{-9}-1.55×10^{-9} esu and 0.003×10^{-8}-1.22×10^{-8} esu. They suggested that it is a good contender to be used in optoelectronic applications.

Akkaya (2018) was fabricated Au/n-GaAs devices with and without organic interface layer (Methylene blue). He used n-type LEC GaAs wafer Te - doped with doping concentration 2-$5 \times 10^{17} cm^{-3}$. Ohmic metal contacts of Au-Ge alloy deposited by thermal evaporation method with thickness of 200 nm, a thin film of MB was deposited on the wafer by spin coating method with thickness of 12.8 nm, and the high purity Au metal was deposited by rapid thermal evaporation method through molybedenum shadow mask with a thickness of 30 nm. All the electrical measurements were applied at room temperature and in dark by using I-V measurements. He reported that the

forbidden band gap of MB film was 1.62 eV and barrier height values were recorded 0.95±0.008 eV and 0.782±0.005 eV with and without MB interlayer respectively. He pointed to that this increasement in barrier height is due to the MB layer, also this MB layer between Schottky metal and GaAs affects the current transportation mechanism at high reverse bias region, and the interface state density values of the Au/MB/GaAs devices were lower than that of Au/GaAs device because of organic dye layer.

3. THE PHYSICS OF ORGANIC SEMICONDUCTORS

3.1. Introduction

At the beginning of 21st century, we are facing a new electronics revolution that has become possible due to the development and understanding of a new class of materials, commonly known as *organic semiconductors*. There are two major classes of organic semiconductors, polymers and low molecular weight materials. The properties of organic materials depend sensitively on the atomic structure of the molecule and the morphology of the materials. Before introducing appropriate methodologies to deal with the dynamic, electronic, and charge transport properties in such materials, it is necessary to understand the basic aspects about how the molecular structure are constituted, and how chemical bonding such as π-system of organic electronic molecules is formed (Radke, 2011).

The charges transport through an organic semiconductor dose not depends only on the nature of the molecular conjugation systems but also on the deformation of the molecular architecture. In this chapter presents of rudimentary introduction to the chemical physics of the organic semiconductors, which represent the basis for understanding the electronic properties of the organic electronic devices. The discussions of this chapter are based on the Refs (Radke, 2011), Podzorov et al. (2004), Coropceanu et al. (2007), Brédas et al. (2002), Valeev et al. (2006), Thorsmølle et al. (2009).

3.1.1. Materials of organic semiconductor

Organic semiconductors are a field of organic materials that include hydrocarbon molecules with a backbone of carbon atoms, which shows desirable electrical conductivity properties falls between insulators and metals. The attractive properties of these materials include their electrical conductivity that can be varied by the changes of temperature, optical excitation and concentration of dopants relative to metal materials, they have mechanical flexibility, and thermal stability.

Organic materials are divided into two main categories, polymers and small molecular materials (Stella, 2009). Chemically there is a big difference between these two kinds of organic materials. Polymeric are macromolecules constructed by the repetition of a fundamental unit known as monomers, which are soluble in organic solvents, hence small molecules are in some cases named molecular materials, are constructed of small molecules and can be divided in to sub groups include Monomers, Dimers, Oligomers and Pigments, which are not soluble in organic solvents, the other sub group is dyes which are soluble in organic solvents (Al-Ghamdi, 2009).

There are significant difference between the processing of semiconducting polymers and small molecule of organic semiconductors, polymers can be solution processed, for example molecules being spin-coated from a solution of appropriate organic solvents, while small molecule materials are quite often insoluble and mostly are thermally evaporating (Stella, 2009). Within the framework of this chapter, it will focus on small molecules, the second class of organic materials.

3.1.2. Chemical bonding in organic molecules

The organic materials are composed mainly of carbon atoms more than of the other elements because of the ability of carbon atoms to bond together to form a wide range of chains and rings (Carey and Sundberg, 2007).

The atomic orbital model shows the probability of finding an electron around the atoms nucleus, and it gives the basic fundemental bulding blocks of the atomic orbital model. The two most interesting kind of atomic orbitals in organic electronics are the *s* orbitals, which are sphere shaped, and the *p* orbitals, which resemble dumbbells with their two ellipsoid shaped lobes that are separated by a nodal plane at the nucleus (Figure. 3.1)
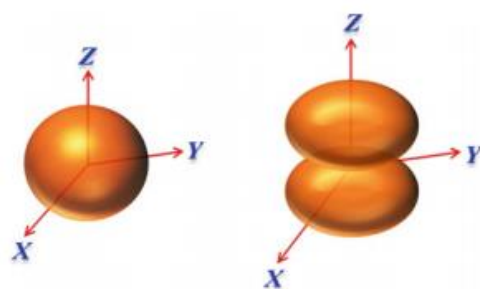
Fig. 3.1. Illustrations of an *s* orbital (left) and a *p* orbital (right), Dey et al. (2015).

The electrons in the outermost shell, the so-called valence electrons, determine the chemical, electrical, and optical properties of materials. They also participate in the formation of chemical bonds with other atoms, Dey et al. (2015).

The electronic configuration of carbon atom is $1s^2\ 2s^2\ 2p_x^1\ 2p_y^1$, which means that two electrons are in 1*s* shell and four valence electrons are in 2*s* and 2*p* subshells which are avilable to form chemical bonds (Stella, 2009, Nassajy, 2015). The subshell 2p consist of three orbitals $2p_x$, $2p_y$ and $2p_z$, this 2p subshell holds up to six electrons but in carbon atom only two electrons are in this subshell, which means that four of the valence electrons residing in 2*s* and 2*p* levels, which can be denoted as $2s^2$ and $2p^2$ respectively (Braun, 2007).

In order to understand electronic configuration in different compounds involving carbon, the theory of valence orbitals hybridization is used. Hybrized orbitals are assums that, one *s* electron is ascend to the last free *p* orbital, thus four singly occupied valence orbitals obtain. The numbers of *p* orbitals which used in the hybridization process defines the type of polymer and many of chemical and structural properties (Carey and Sundberg, 2007),

Both kinds of organic materials polymers and small molecules have in common a conjugated π-electron system formed by p_z orbitals of sp^2 hybridized carbon atoms in the molecules, (Figure 3.2) (Brütting, 2005).
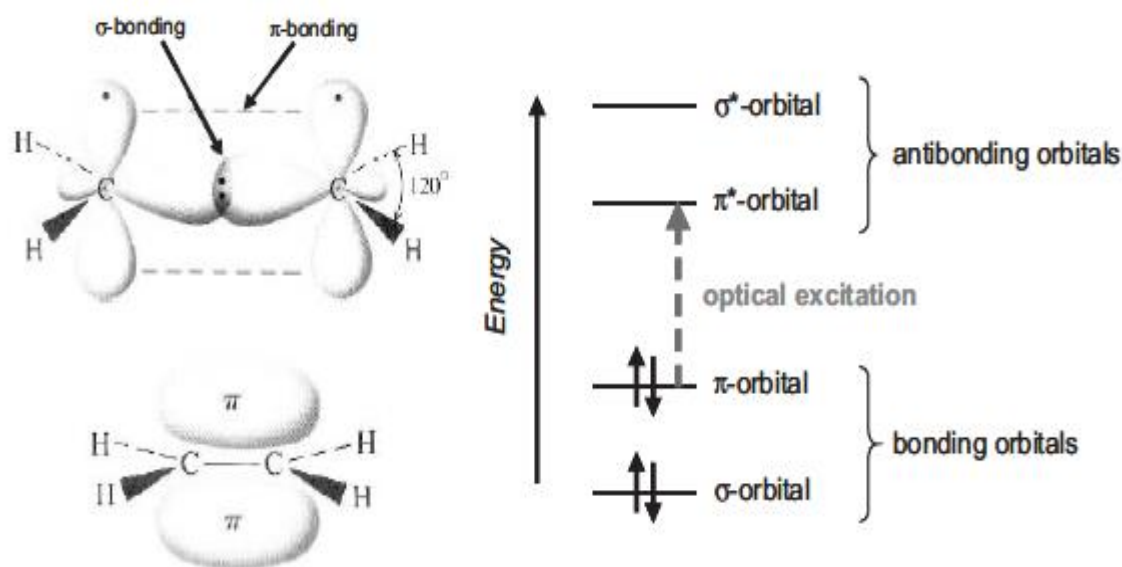
Figure 3.2. Left: σ- and π-bonds in ethene, as an example for the simplest conjugated π -electron system. The right viewgraph shows the energy levels of a π - conjugated molecule. The lowest electronic excitation is between the bonding π -orbital and the antibonding π *-orbital (Brütting, 2005).

When one *s* orbitals mixes with three *p* orbitals, three hybridization orbitals are possible: sp^1, sp^2, and sp^3 for carbon atoms (Nassajy, 2015). In (Figure 3.3) ascheme explains the concept of hybirdization. The new orbitals are linear combinations of the pairing electrons in the atomic carbon orbitals to form different chemical bonds and minimise the total energy of the formed compound (Braun, 2007). Each sp^3 type hybrid orbitals consist of two lobes of different size, four large lobes are orinted towards the corners of a tetrahedral structure with angles of 109.5°, when carbon atoms are bonded in such arrangement each of them has four neighbors and this configuration can be found in methane. Another type of hybridization is, when one *s* and two *p* atomic orbitals hybridized, the three hybrids are span in the plane and oreinted at angles of 120°, to one another and contains one electron each. The remining electron resides in unhybridized *p* orbital oreinted perpendicular to the plane of sp^2 orbitals, the structure of ethylene is presented as an example of this hybridized configuration.
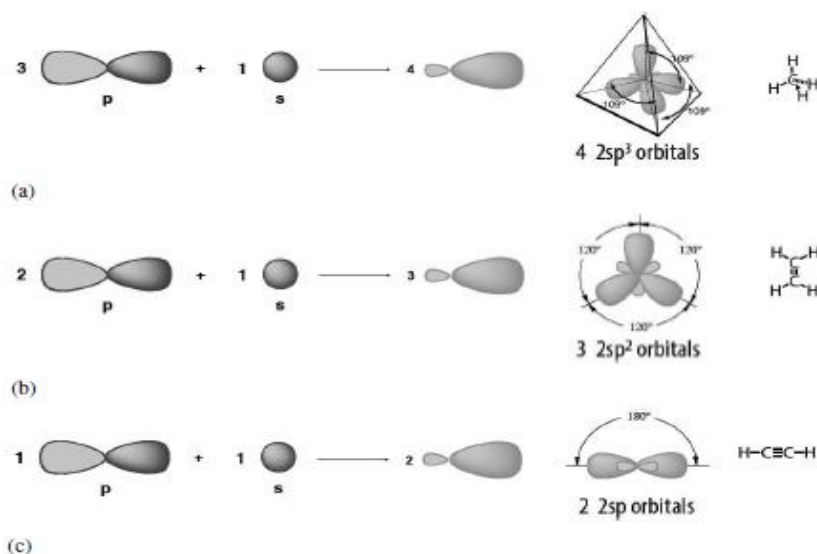
Figure 3.3. Carbon orbital (a) sp^3, (b) sp^2 and (c) sp hybridizations (Nassajy, 2015).

When two atoms of carbon are bound through hybridized orbitals like ethane moleucle as an example, the bonding picture according to valence orbital theory, both carbon atoms are *sp*^{3}-hybridized, which means that both have four bonds arranged with tetrahedral geometry. The carbon-carbon bond is formed by overlaping of one *sp*^{3} orbital form each of the carbon atoms, while the six carbon-hydrogen bonds are formed by overlaping between the remining *sp*^{3} orbitals on the two carbon atoms and the 1*s* orbitals of hydrogen atoms, these bonds are known as sigma bonds and denoted as σ. Because they are formed from the end-on-end overlaping of two orbitals, so they are symmetrical about the axis joining the two nucleies (Figure 3.4) (Braun, 2007).
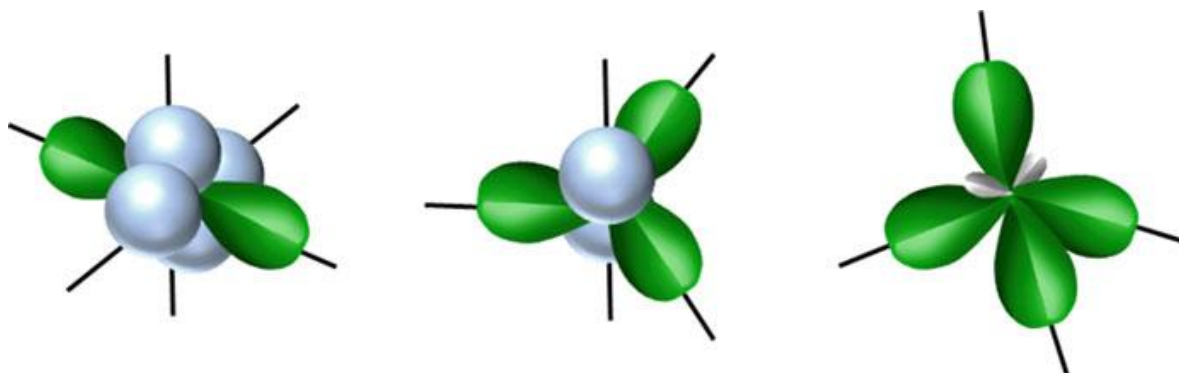
Figure 3.4. Illustrations of sp^1 (left), sp^2 (center), and sp^3 (right) hybridized orbitals (Dey et al. 2015).

A second bond, called a pi bonds and denoted as π is formed by the side-by-side overlap of two unhybridized $2p_z$ orbitals from each carbon and atom and geometrically is perpendicular to the axis joining two nuclei, which does not have symmetrical symmetry and prevents the rotation of the atoms along the sigma bonding direction.

These two typs of bonds differ significantlly by means of their strength, the σ or single bond is the strongest type of covalent bonds with rotational symmetry about the bond axis, while the π bond is usually weaker than σ bond and it is formed where two lobes of residual 2p orbital of one atom overlap two lobes of the other parallel residual 2p orbital of the adjoining atoms, thus π bond have no rotational symmetry around the bond axis. The ethylene molecule for example has one σ and π bond leading to a double bond between the carbon atoms. The electrons in σ and π bonds some times are refered to as σ and π electrons (Nassajy, 2015). (Figure 3.4) As an example, for sigma and pi bonds.
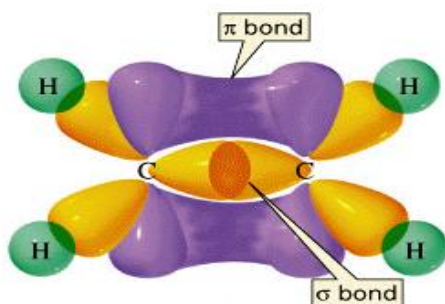
Figure 3.5. A scheme of pi and sigma bond in ethane.

3.1.3. Energy Bands in Orgnic Solid Semiconductor

Beside of various interactions that occurs between neighboring atoms such as orbital hybidizations, when two atoms of carbon are brought together to interact, their energy levels are siplitted, creating two different molecular energy levels, one with lower energy than the original ones and another energy level with higher energy. Such new molecular orbitals called linear combination of atomic orbitals, (LCAO) is an approximation to calculate molecular orbitals, the even or symmetric combination is the bonding orbital, while the odd or antisymmetric combination is called the antibonding

orbital, the antibonding are denoted as σ^* and π^* orbitals for antibonding counterparts (Nassajy, 2015). (Figure 3.5) shows the lower energy bonding orbitals and the higher energy antibonding orbitals, here σ bonds represent the lowest unoccupied molecular orbital (LUMO), onwards are empty, and π bonds are represent the highest occupied orbital (HOMO), are filled with two electrons of antiparallel spin. The diffrence between (HOMO) and (LUMO) corresponding to the energy gap (*Eg*).
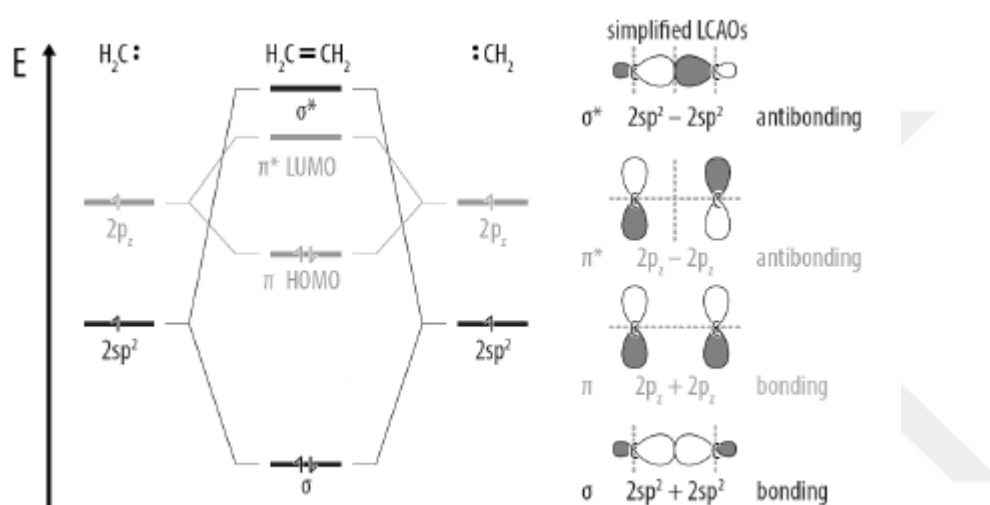
Figure 3.6. The antibonding and bonding orbitals along with the electron energy level
configuration for the ethylene (Nassajy, 2015).

3.3. General Approach To Charge Transfer Mechanisms

Charge transport in organic semiconductors is a timely subject. There is quite a range of charge transfer models based on the molecular picture that are employed to describe charge transport in organic solids, such as models based on band transport, polaronic models, and models that focus on the effects of disorder (Bässler and Köhler, 2011).

To understand the mechanisim of charge transport and conductivity in organic semiconductors, its need to know information about, charge carriers types in organic semiconductors, generation mechanism of charge carriers in organic semiconductors,

recombination mechansim for charge carriers, and charge trapping processes and transport conduction mechansim in organic semiconductors.

Charge carrier types and generation recombination mechansim are mentioned in section 3.2. Energy band in organic solid semiconductors. Here is simply outline of the main characteristics of the most popular models which used to explain transport conduction mechanism models of charge carriers in organic semiconductors.

3.3.1. Hopping transport model of charge carriers.

Presumably in this model that charge carriers transport from location to another by hopping (Figure 3.6a) clearly shows hopping of a charge carriers from molecule 1 to molecule 2, this model is the prevalent mechanism in most organic compounds by (cation-anion) charges, and the diffusion of the transporation happen by (oxidation − reduction) reactions. In this model, the exchange of energy of the electrons is less compared to the energy of the reaction of (electron-phonon), but more than differentiate energy of phonons, and according to this model charge carrier can be trapped in any location in the molecule and moving over the barriers between the molecules by activating energy. It must be recognize between charge transport from one location to another along the π bonds of the molucle and the transfer of the charge molecule chain to another adjacent molucle chain see (Figure 3.6b) where the first type is more efficient (Stella, 2009, AL-Ghamdi, 2009).

3.2.2. Quantum mechanical tunneling model.

In this model π electrons transfer from one moeclule to another adjacent molecule by tunneling, it can be imagine that through two steps. First step is excitation of single molecule by heat or light to form an electron in the first excitation level in the lowest unoccupied molecular orbital LUMO leaving a hole in the highest occupied molecular orbital HOMO which consist of energy levels, each level occupied by two electrons. Second step represents transfer of charge carriers (electron or hole) by tunneling through the energy barriers between molecules from the original molecule to

the same energy level in the adjacent molecule (Shinar and Shinar, 2009, AL-Ghamdi, 2009).

3.2.3. Band energy transport model.

According to this model the charge carriers in the organic semiconductor which have a mobility will get drift motion in the material depends on temperature through the relation

$$\mu \propto T^{-n} \quad with \quad n = 1 \dots 3$$

Where μ is the mobility of charge carriers, it is observed that beside of the weak mobility of the charge carriers, its mobility is also dependents on the density of the electrical field F through Poole – Frenkel formula.

$$\mu = \mu_0 \, exp(\gamma \sqrt{F})$$

Here, μ_0 is the zero-field mobility, γ is a field activation parameter and E denotes electrical field (Bässler and Köhler, 2011, Coropceanu, 2007). Where the mobility of charge carriers in organic semiconductors is often very little, about 10^{-2} cm^{-2}/V.s in perfect chain of conjugated polymers as a sequence of molecular repeat units such as liquid crystalline in Polyfluorene and arrives to 10^{-8} cm-^{2}/V.s in (host-gust) conjugated polymers systems such as dye doped Poly-vinylcarbazol. It is possible to increase the mobility of charge carriers by applying an electric field E, also the mobility is increased many orders when the molecules arrenged perfectly in the matter, so the single organic molecule has the best performance because of its highest mobility, the mobility of charge carriers decreased by defects or impurities (traps) (Braun, 2007). In this model of charge carrier transfer the mean free path of the carriers must be greater than crystal lattice constant, and the mobility of the carriers greater than $3W/k_BT$ where W is band width which must be greater than vibration energy of the lattice. For organic semiconductors, $W \approx 10$ kT and $a \approx 1$ nm so that band transport occurs if $\mu \approx 10$ cm^2 V^{-1} s^{-1}. İn this model the prevailing exchange method of energy between the electrons and crystal lattice is through (electron-phonon) reaction or through phonon dispersion energy (Bässler and Köhler, 2011).

Band transport model is used commonly to describe electrical conductivity of semiconductors in general according to band theory, but in most more than one model were mentioned is used to describe the mechanism of electrical conductivity of organic semiconductors, generally the conductivity in most are exponential formula and electrical conductivity applied as a function of temperature dependences of the conductivity of the organic semiconductor and is given by the formula

$$\sigma = \sigma_o e^{\Delta E_a / kT} \tag{3.2}$$

Where σ_o is intrinsic conductivity of charge carriers, and ΔE_a is activation energy for charge carriers.

The simplified application of band theory suppose that ΔE_a is equvalent to band gap energy *Eg*, and this is true just for high purity materials, which have intrinsic conductance, but in less purity material or materials which conatine dopants, traps or defects, the value of ΔE_a is relative to different casual conduction mechanism, also the experimental values of ΔE for organic material depends on crystalline states beside of the purity of the material, where the mobility is decrease by to orders at least because of impurities or traps and defects (AL-Ghamdi, 2009, Ayala, 2013).
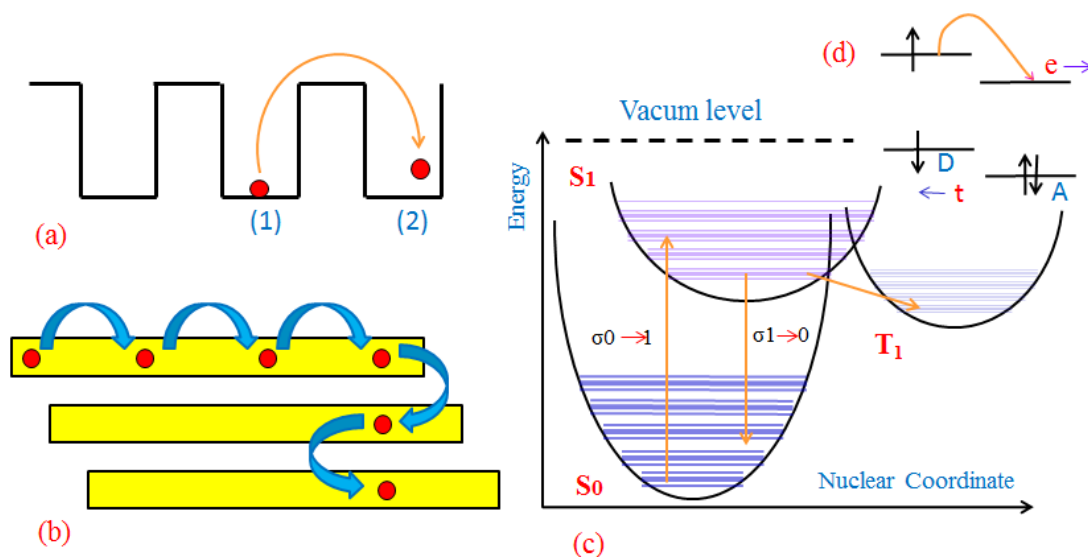
Figure 3.7. Schematic of charge transport mechansims (a) charge carrier hopping process between two moleculs(1) and (2), (b) Internal transmitting of charge from one location to another in same molecule. (c) transmitting associated with absorption S_0 to S_1, and fluorescence S_1 to S_0 and inter system transverse crossing process (ISC) S_1 to T_1(AL-Ghamdi, 2009).

3.3. Phenol Red

Phenol red (phenolsulfonphthalein = PSP) is an organic dye are classified under small molecules organic materials, the molecular formula of phenol red is $C_{19}H_{14}O_5S$, the chemical structure contains in total of 42 bonds, which include 28 non-H bonds, 20 multiple bonds, 2 rotatable bonds, 2 double bonds, 18 aromatic bonds, 1 five rings, 3 six-membered rings, 1 nine-membered rings, 2 aromatic hydroxyls and 1 sulfonate, (Figure 3.7).

Phenol red exists as a red crystal that is stable in air; its solubility is 2.9 g/l in ethanol and 0.77 g/l in water. Phenol red color changes gradually from yellow to red then pink with changes of pH. In solution (low pH) and in crystalline form, the compound exists as zwitterion. Formerly a zwitterion called a dipolar ion in chemistry. Zwitterion is a molecule with two functional groups, of which one has a negative and one has a positive electrical charge and the net charge of the entire molecule equals to zero. The charges on the different functional groups balance each other out, and the molecule as a whole is electrically neutral. This zwitterion property of phenol red simultaneously has both ionic states which called cationic and anionic. The ketone group carrying an additional proton (positive charge), and the anion group is carrying a negative charge. These ketone-anion groups are involved in charge carriers transport mechanism in this organic dye.
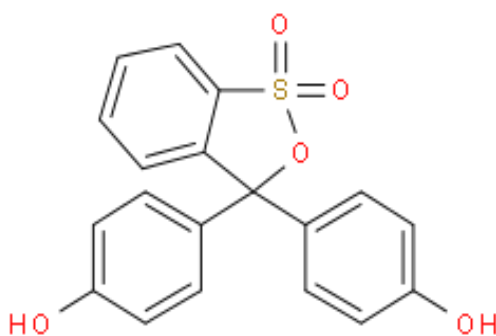
Figure 3.8. Phenol red (Phenolsulphonphthalein) chemical structure.

4. MATERIAL AND METHOD

4.1. Metal-Semiconductor Contacts

When a metal and a semiconductor are joined, two different possible types of contacts can be produced which depends on the type of the metal and the semiconductor (Sze and Ng, 2006).

The contact with non-linear, rectifying current-voltage characteristics is called a Schottky contact which allows current to pass only in one direction. Linear non-rectifying current-voltage contact is called an Ohmic contact, which allows current to flow in either direction of the junction (Colinge and Colinge, 2005).

This chapter is analyzed the electrical characteristics of both rectifying and Ohmic contacts, and the discussion is totally about the p-type semiconductors.

4.1.1. Rectifying contact

A rectifying contact or Schottky barrier diode is formed by joining a metal with a p or n-type semiconductor. It is necessary to introduce the concept of work function, before discussing the behavior of metal-semiconductor contacts. Work function of a metal, $q\Phi_m$, is defined as the minimum energy required to extract one electron from E_{FM} (the metal Fermi level) of the metal. Similarly, the work function of the semiconductor $q\Phi_s$ is the energy required to extract an electron located at its valence level (Figure 4.1a) (Colinge and Colinge, 2005).

After thermal equilibrium, the work function is the difference between the vacuum level and the Fermi level energies, and it is expressed by (Sze, 2008).

$$q\Phi_{m=}Eg + q(\chi + V_n) \tag{4.1}$$

Where Eg is the band gap energy of semiconductor, $q\chi$ is the energy needed to extract an electron from the conduction band Ec in to a vacuum level is called electron affinity (4.01 eV for Si), and qV_n is the energy difference between conduction band Ec, and the Fermi level E_F (Sze and Ng, 2006).

The values of work functions are very sensitive to surface contamination. Typical values of work function for very clean surfaces are 4.3 eV for Al and 4.8 eV for Au metal (Sze, 2008, Nassajy, 2015).

When a metal with a work function $q\Phi_m$ is connected to a p-type semiconductor having a work function $q\Phi_s$, thermodynamic equilibrium is established through the transfer of positive charge from the semiconductor to the metal and the Fermi levels align, Figure 4.1b. (Sze, 2008).
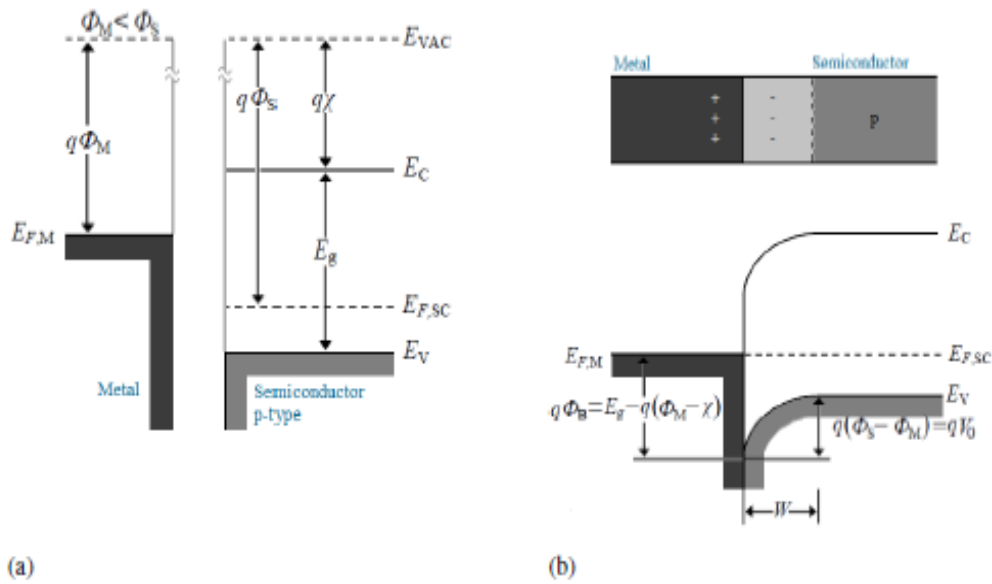
Figure 4.1. Schottky barrier between a metal and a p-type semiconductor having a greater work function: (a) band diagrams before joining; (b) band diagrams after joining at equilibrium. E_{VAC} is the vacuum energy level, $q\Phi_m$ is the metal work function, $E_{F,M}$ is the metal Fermi energy, $E_{F,SC}$ is the semiconductor Fermi energy, $q\chi$ is the semiconductor electron affinity, Ec is the semiconductor conduction band edge, Ev is the semiconductor valence band edge, $q\Phi_B$ is the Schottky barrier energy, W is the depletion region and V_0 is the contact potential. (Nassajy, 2015).

When $\Phi_M < \Phi_s$, Fermi level of semiconductors is initially lower than that of the metal, before the contact is formed. For alignment of the Fermi levels between the metal and the semiconductor, the electrons energy of the semiconductor must be raised relative to the electrons energy of the metal. It results in the form of a constant equilibrium potential difference (V_o) between the metal and the semiconductor (Mishra and Singh, 2007). A space-charge region corresponding to the zone depleted of

electrons is formed in the semiconductor near the interface between the junction, the width of this depletion zone is denoted W (Colinge and Colinge, 2005).

$$W = \sqrt{\frac{2\varepsilon_\circ \varepsilon_r (V_0 - V)}{q N_A}} \qquad (4.2)$$

where ε_o is the permittivity of vacuum, ε_s is the relative permittivity of the semiconductor, V_0 is the contact potential, V is the external applied voltage, q is the elementary charge and N_A is the density of dopants.
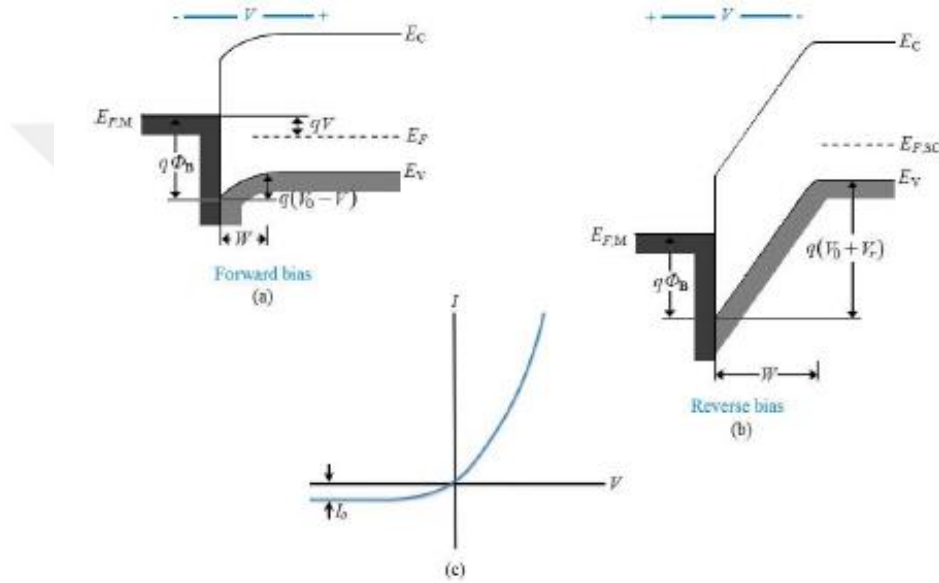
Figure 4.2. Effects of forward and reverse bias on the junction of Figure 4.2: (a) forward bias; (b) reverse bias (V = -Vr); (c) typical current-voltage characteristic (Nassajy, 2015).

In the depletion region the holes are transit from one side of the junction to the other side. Some holes diffuse from the semiconductor to the metal, and some other holes are swept by the electric field from the metal to the semiconductor (Nassajy, 2015). At thermodynamic equilibrium, and in the absence of any external bias, the contact potential V_0 prevents further net hole migrating from the semiconductor conduction band in to the metal side, and (V_o) is equal to the difference of the tow work functions

$$qV_0 = q(\Phi_{S-}\Phi_M) \qquad (4.3)$$

Thus, the potential barrier V_o having an amplitude equal to

$$q\Phi_b = q(\Phi m - \chi) \tag{4.4}$$

Figure (4.1) (Colinge and Colinge, 2005). However, the V_o can be decreased or increased by the application of the either forward or reverse bias voltage (V) across the junction figure 4.2. (Nassajy, 2015).

4.1.2. Ohmic contact

An Ohmic contact is a non-rectifying contact (Colinge and Colinge, 2005), this metal-semiconductor contact has a negligible contact resistance relative to the bulk or series resistance of the semiconductor (Sze and Ng, 2006, Sze, 2008). The current-voltage characteristics of the contact obey the Ohmic law which is linear in the both biasing direction (Colinge and Colinge, 2005). Typical *I-V* characteristics of an Ohmic contact are shown in (Figure 4.3) (Ng, 2002). Linearity of these characteristics is not important as long as they provide adequate current with small voltage drop. (Ng, 2002). The specific contact resistance is reciprocal of the derivative of current density with respect to voltage, R_C defined as (Ng, 2002, Mishra and Singh, 2007, Sze and Ng, 2006, Sze, 2006; 2008).

$$R_C \equiv \left(\frac{\partial I}{\partial V}\right)_{V \Rightarrow 0}^{-1} \Omega - cm^2 \tag{4.5}$$

For metal-semiconductor contacts with low doping concentrations, the thermionic-emission current dominates the current transport, as giving by Eqs

$$I = I_0 \left(e^{qV/kT} - 1\right) \tag{4.6}$$

therefore,

$$R_C \equiv \frac{k}{qA^*T} exp(\frac{q\Phi_{Bn}}{kT}) \tag{4.7}$$

Equation 4.7 shows that a metal-semiconductor contact with a low barrier height should be used to obtain a small R_C (Ng, 2002, Colinge and Colinge, 2005, Sze, 2008, Mishra and Singh, 2007, Sze and Ng, 2006).

For an Ohmic metal-semiconductor contact, the charges transfer from the metal to the semiconductor in aligning the Fermi levels. For a p-type semiconductor, this

happens when $\Phi_M > \Phi_s$, the Femi levels are aligned at equilibrium by transferring holes from the metal to the semiconductor. This lowers the energy levels of the semiconductor relative to the metal at equilibrium conduction (Figure 4.3a). This lowering of the barrier makes flowing of the holes between the metal and semiconductor easily overcoming under small voltage (Ng, 2002, Nassajy, 2015, Sze and Ng, 2006).

In a particular case of $E_{FM} < E_{FS}$ such that the energy bands of the p-type semiconductor are bends towards near the contact. The magnitude of the band bending and its extension in to the metal are very small. As a result, the potential barrier is small for hole transport between the metal and the semiconductor and holes can flow and easily overcome through the contact by a small voltage. Such contact is ohmic (Figure 4.3b).
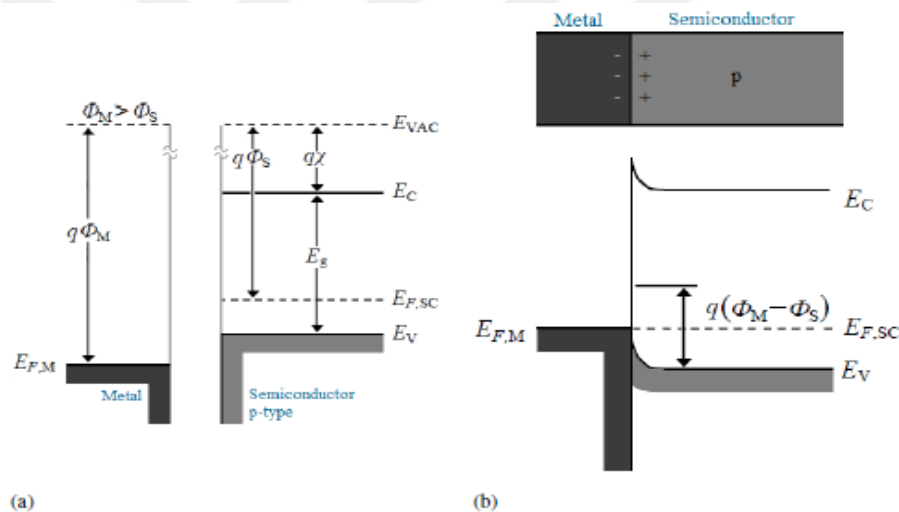
Figure 4.3. Ohmic contact between a p-type semiconductor and a metal having a greater work function: (a) band diagrams before joining; (b) the equilibrium band diagram for the junction. (Nassajy, 2015).

The current components through an ohmic contact are different. in field emission (FE), carriers' tunnel at an energy near the Fermi level. In thermionic-field emission (TFE), the carriers are tunnel at an elevated energy, where the barrier becomes narrower. In thermionic emission TE, carriers do not tunnel, but they are emitted thermally over the barrier. This mechanism is identical to a regular Schottky-barrier current conduction (Ng, 2002)

In practice, a Schottky contacts behaves as an ohmic contact, if the impurity concentrations in the semiconductor is high enough (e.s $N_d=10^{20}$ cm^{-3}) (Colinge and Colinge, 2005). Electrons can easily tunnel through such a thin potential barrier, which yields a low Ohmic resistance between the metal and the semiconductor. In metal-to-silicon contacts, current flow by tunnel effect becomes larger than the current flow by thermionic emission, when doping concentration is larger than 10^{17} cm^{-3}. In practice, ohmic contacts between a metal and the terminals of semiconductor devices are always made on heavily doped areas (Ng, 2002, Colinge and Colinge, 2005, Sze, 2008, Mishra and Singh, 2007, Sze and Ng, 2006).

4.2. Definition of Electrical Parameter of Devices

4.2.1. Barrier height

The barrier height of metal-semiconductor systems are, in general determined by the metal work function and the surface state.

In an ideal Schottky barrier diode with no band gap defect levels, the height of the barrier at the metal-semiconductor junction is defined as the difference between the semiconductor conduction band at the junction and Fermi level of the metal. This barrier is given by Eq 4.4.

Similarly, for the case of an ideal contact between a metal and p-type semiconductor, the barrier height $q\Phi_{bp}$ is given by (Mishra and Singh, 2007).

$$q\Phi_{bp} = Eg - q(\Phi m - \chi) \tag{4.8}$$

where Eg is the band gap of the semiconductor (Sze, 2008). The coming electrons from the semiconductor in to the metal face a barrier denoted by qV_o as shown in (Figure 4.3b) . The potential qV_o is called the built-in potential of the junction, and is given by (Mishra and Singh, 2007).

$$qV_o = (q\Phi_s - q\Phi_m) \tag{4.9}$$

For metals with work function $\Phi_M < \Phi_s$, it is possible to have a barrier for hole transport between a metal and p-type semiconductor junction. In this case at equilibrium

the electrons are injected from the metal to the semiconductor, leaving a negative charge in the semiconductor side. The energy bands are bent and a barrier is created for the holes transport (Sze, 2008).

The Schottky barrier height for n-type or p-type semiconductor depends upon the metal and the semiconductor properties, this for an ideal case. Experimentally it is found that the Schottky barrier height is often independent on the metal used. The Schottky barrier is indeed controlled by the metal work function and the interfacial properties (Ng, 2002, Mishra and Singh, 2007).

When a forward-bias voltage V is applied to the Schottky barrier fig (3-6 b) (Ars), the potential of the contact is decreases from V_0 to $V_0 - V$ fig (3-7a) ars. As a result, holes in the valence band of the semiconductor can diffuse across the depletion region to the metal. This raises the forward current from the semiconductor to the metal through the junction. Conversely, a reverse bias increases the barrier to $V_0 + V_r$, and the holes flow from the semiconductor to the metal are become negligible fig (4-3 b). In either case of holes flow from the metal to semiconductor is hampered by the barrier Φ_B, which is not affected by the bias voltage. The current transport in a Schottky barrier is due to mainly majority carriers, for Schottky diodes which is operated at moderate temperature about (e.g., 300K), the dominate transport mechanism is thermionic emission of the majority carriers from the semiconductor over the potential barrier in to the metal (Colinge and Colinge, 2005).

The resulted current of the diode is shown in fig (4.3b). The reverse saturation current (I_o) depends on the barrier height for holes injection from the metal to the semiconductor, the Schottky barrier diode can rectify, with flowing easily for the current in forward bias and small current flowing in reverse bias. Because of the dependence of the potential barrier height on the applied bias and because of generation /recombination in the depletion zone the forward current takes this form (Colinge and Colinge, 2005).

$$I = AA^* exp\left[\frac{-q\Phi b}{kT}\right][exp\ \left(\frac{qV}{nkT}\right) - 1] \tag{4.11}$$

where $1 \leq n \leq 2$ is called the ideality factor of the diode, A^* is called the effective Richardson constant, it $(4\pi q k^2 m_e/h^3)$. k_B is Boltzmann constant (1.38x10^{-23} J/K) and

T is the absolute temperature. The value of A^* is equal to 32, for p-type Si (Colinge and Colinge, 2005). The forward current is due to the injection of the majority carriers from the semiconductor in to the metal. There is no minority carrier injection, so the storage delay time associated with the minority carrier injection is absent in Schottky barrier diodes. The high-frequency properties and switching speed are in Schottky barrier generally better than typical p-n junctions (Nassajy, 2015).

4.2.2. Modified Norde function

Some methods, which have been proposed, allow the determination of the diode parameters. A modified Norde function is used to determine the series resistance and barrier height from *I-V* measurement of a Schottky barrier diode Schroder, 2015).

In order to make an accurate determination of Schottky diode parameters such as ideality factor, barrier height and the series resistance using forward current-voltage *I-V* characteristics in the presence of an interfacial layer, a novel calculation method has been developed by taking in to account the applied voltage drop across the interfacial layer (V_i) (Sze and Ng, 2006). The approach involves the use of an auxiliary function and computer-fitting routine. This technique has been found to be both accurate and reliable (Ng, 2002). In this model of calculation, the properties are derived at any forward bias voltage from the current-voltage characteristic, and its first and second derivative. The *I-V* characteristics of a Schottky diode are given by:

$$I = I_o \exp(\beta\Phi) \left[\exp\left[\frac{\beta(V-IR)}{n} \right] - 1 \right]$$ (4.12)

Where

$$I_o = AA^*T^2(-\beta\Phi)$$ (4.13)

where $= \frac{q}{k_B T}$. The saturation current I_o is independent of voltage. Assuming the ideality factor to have a value of $n = 1$, Norde developed the following function for extracting parameters Φ_b and R_s of Schottky contacts (Norde, 1979, Donchev, 2015).

$$F(V) = \frac{V}{2} - \frac{1}{\beta} \ln\left(\frac{I}{I_o} \right)$$ (4.14)

In the proposed method, it is assumed that

$$F(V) = \frac{V}{\gamma} - kT/q\left(\frac{I(V)}{AA^*T^2}\right) \tag{4.15}$$

where γ is the first integer greater than ideality factor value obtained from *I-V* calculation, and $I(V)$ is the current value obtained from *I-V* curve. Barrier height can be calculated by using the minimum value of the plot of F(V) vs. *V* using this equation (Norde, 1979)

$$\Phi_B = F(V_{min}) + \frac{V_{min}}{\gamma} - \frac{kT}{q} \tag{4.16}$$

where F(V_{min}) is the minimum of $F(V)$ curve and V_{min} is the corresponding voltage value. The series resistance of the device can be calculated through the relation (Taşçıoğlu et al, 2013, Gromov and Pugachevich, 1994).

$$R_s = \frac{kT}{qI_{min}}(\gamma - n) \tag{4.17}$$

Where I_{min} is the corresponding current value at V_{min}.

4.2.3. Cheung-Cheung method

Fundamental parameters of the Schottky diode, which are barrier height Φ_b, ideality factor *n* and series resistance R_s, are determined from the forward *I-V* characteristics by using Cheungs' functions. Cheung functions present an alternate approach to determine the values of *n*, Φ_b and R_s from a single *I-V* data, by written equation (1) in terms of current density$(I = \frac{I}{A_{eff}})$. Thus

$$V = RA_{eff}I + n\Phi_b + \left(\frac{n}{\beta}\right)\ln\left(\frac{I}{A^*T^2}\right) \tag{4.18}$$

where $\beta = \frac{q}{kT}$

Differentiating Eq. (4.18) with respect to *I*, and rearranging terms, Eq (4.19) obtained

$$\frac{dV}{d(\ln I)} = RA_{eff}I + \frac{n}{\beta} \tag{4.19}$$

Calculating Φ_b can be determined by *H* (*I*) function as given in Eqs

$$H(I) \equiv V - \left(\frac{n}{\beta}\right) \ln\left(\frac{I}{A^*T^2}\right) \tag{4.20}$$

For Eq. (4.18), it can be written as

$$H(I) \equiv RA_{eff}I + n\Phi_b \tag{4.21}$$

By using the value of n from Eq.(4.19), a plot of $H(I)$ vs I also gives a straight line with y-axis intercept equal to $n\Phi_b$ (Cheung, 1986). The slope of this plot also provides another determination of R_s, which can be used to check the consistency of this approach. Thus preforming to different plots Eqs (4.19) and (4.21) of I-V data obtained from same measurement can calculate all the three key diode parameters n, Φ_B and R_s (Benhaliliba et al,2014).

4.3. Spin Coating Technique

Spin coating is one of the most common techniques for applying thin films to substrates especially liquid solutions of materials. It is used in a wide variety of industries and technology sectors. The advantage of spin coating is its ability to quickly and easily produce very uniform films on flat substrates. The use of spin coating in organic electronics and nanotechnology is widespread and has built upon many of the techniques used in other semiconductor industries (Manikandan et al,2015).

4.4. Thermal Vacuum Evaporation

Thermal Evaporation is a common method for thin-film deposition of purified materials. The source material is evaporated in a vacuum. The vacuum allows vapor particles to travel directly to the target object, where they condense back to a solid state.

Thermal evaporation of small molecules is usually performed in a vacuum of $\sim 10^{-6}$ Torr. However, it has been observed that the residual gases in the chamber may affect the performance of the devices significantly. This was apparently due to the

formation of an oxide buffer layer between the top organic layer and the metal cathode, indeed led to the creation of an AlO_x buffer layer.
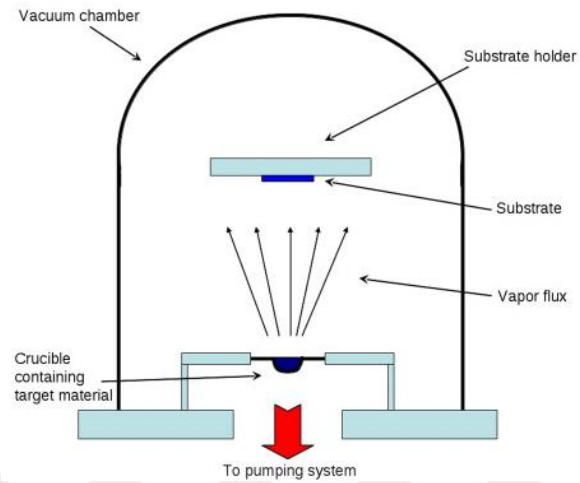

Figure 4.4. Schematic of a typical thermal evaporation system. The source material is heated by an electrical current in thermal evaporation.

5. EXPERIMENTAL PROCEDURE

5.1. Introduction

In this chapter, the fabrication and electrical characterization of metal /PSP/p-Si organic diodes are investigated. Five different metals Ag, Cu, Ni, Pd and Sn with different work function were used as a top contact metal in the fabrication of heterostructure with and without organic interlayer of phenol red (phenolsulfonphthalein = PSP). Based on the analyzing of the current-voltage data, and capacitance-voltage data, main electronic parameters such as ideality factor n, barrier height Φ_b, and series resistance R_s are determined for the studied Schottky barriers. For a better understanding of the effect of the phenol red as an organic layer, and the different metal work function on the electrical properties of the studied devices, different measurements and calculation methods, are performed to compare/verify the values of electrical parameters of devices.

The performance of the Schottky diodes with thin interfacial organic layer depends on the charge injection and collection properties of the metal contact electrodes. One of the ways to enhance the good feasibly Schottky barrier is to inserting an organic interfacial layer. The possible method for organic semiconductors is to use the metal with the appropriate work function for better performance.

5.2. Formation of The Samples

In this work, the samples are prepared on p-Si (100) orientation wafer and (1-10) Ω-cm resistivity with and without organic layer.

5.2.1. Cleaning processing of the samples

Cleaning processing of the samples by chemical solutions were applied before processing the wafer. Firstly the wafers dipped in Methanol solution and later in

acetone. Then, the samples were putted in ultrasonic machine for extra cleaning for 5 min at $25^{o}C$, then washed by deionized water and released in to acetone for 5 min at $25^{o}C$. Then, the wafers bathed in deionized water and cleaned by HF (Fluoric acid) with concentration 1:10% with deionized water for several seconds. Then, the wafers were left in air to dry and ready to next steps.

5.2.1. Formation of the ohmic contact

After the cleaning processing, the Ohmic contact was made by thermally evaporating of Al metal on the back surface of the precleaned substrate, and then samples with Ohmic contacts were annealed at 570 ℃ for 3 min in a nitrogen atmosphere.

5.2.2. Deposition of phenol red thin film

After cleaning process 7 mg of phenol red (Soluphonsolfthylien= PSP) powder with 20ml methanol were mixed to form a solution, and stirred for 1 hour. This solution are deposited on the p-Si using spin coating technique at 1000 rpm for 1min, $1\mu l$ of the solution was added in this process to form thin layer of Phenol red on each wafer.

5.2.3. Formation of front contact

Five different metals were used to form the top contact of the diodes by thermal evaporation technique. Shadow mask with diameter about 1mm was used for Ag, Cu, Ni, Pd and Sn metals. All evaporation processes were carried out in a vacuum coating unit at (10^{-6} Torr) pressure.

5.3. Device Structure

The organic Schottky diode is composed of two metal electrodes and a p-type semiconductor covered with organic thin film sandwiched amid the p-Si and metal contacts.

In this work, the diodes are vertically fabricated. The schematic diagram of two dimentional sandwich structure is presented in Figure 5.1.
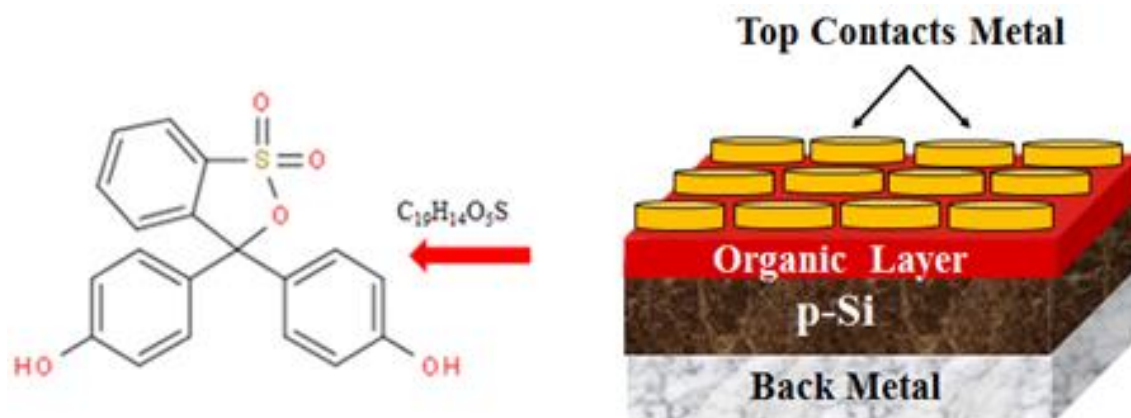
Fig 5.1. a). Molecular structure of PSP and b) Schematic diagram organic-based device structure.

As Figure 5.3 illustrates the organic Schottky diode structure, in this work consist of aluminum as back metal electrode and Ag, Cu, Ni, Pd and Sn as contact metal electrode enfolding the phenol red (phenolsulfonphthalein=PSP) as an organic thin layer, where all these thin films have been layered successively, with diameter of 0.4 mm and 0.5 mm for each top contact.

6. RESULTS AND DISCUSION

6.1. Introduction (Measurement of electrical parameters)

Basically to measure electrical parameters of MS diodes, four methods can be uses; these methods are current-voltage, capacitance-voltage, activation energy and photoelectric methods (Sze and Ng, 2006).

In this work, the following measurements are performed to determine main electrical properties of M/p-Si diodes as a references, and with an organic phenol red interlayer M/PSP/p-Si diodes, were (M=Ag, Cu, Ni, Pb and Sn). Using obtained results the effect of phenol red thin film and the work function of each metal on the properties of prepared diodes were determined.

6.2. Current-Voltage Measurements of Diodes

The *I-V* properties of metal/p-Si and with a PSP organic thin film were carried out in both biasing voltages using Keithley-2400 SCS instrument. The measurements were performed under sweep of bias voltage from -2V to +2V. The curves of *I-V* data for diodes with and without organic layer for the five different metal contacts are shown in (Figures 6.1 to 6.5). From these figures, the experimental semi logarithmic *I-V* plots, the diodes exhibit rectifying behavior. According to figures this feature, it is seen that the diodes exhibit Schottky diode property. To find the electrical properties of diodes, it is possible to use thermionic emission theory (Ozaydin and Akkilic, 2014). Beside the other electrical properties, rectifying factor (*R)* is calculated from the ratio of current at 1V and -1V, as listed in Table (6.1) for fabricated samples. This ratio is given through Eq

$$R = \frac{I(1V)}{I(-1V)} \tag{6.1}$$

The current (I) is expressed according to thermionic emission theory as following Eqs (Sze and Ng, 2006).

$$I = I_o exp\left(\frac{qV}{nkT}\right)$$ (6.2)

Where I_o saturation current derived from Eq. (6.2) and from the intercept section of the straight line in I-V plot when the bias voltage was zero, as it given by Eq

$$I_o = AA^*T^2 exp\left[\frac{-q\Phi_b}{kT}\right]$$ (6.3)

For p-type Si, the effective Richardson constant A^* is equal to 32 A/cm^{2}K^2,. (Verma et al, 2011). By rearranging of Eq 6.3

$$\ln I = \frac{I_o qV}{nkT} - \ln I_o$$ (6.4)

This plot would be linear and therefore by taking the tangent of this linear section of the I-V curve and extrapolating it to cross the y-axis saturation current I_o will gives, see Figures (6.1 to 6.5), whilst the ideality factor n can be getting from the gradient as in Eq.

$$n = \frac{q}{kT}\left(\frac{dV}{d(\ln I)}\right)$$ (6.5)

Rearranging Eq. (6.3) provides to found the barrier height as given in following Eq.

$$\Phi_b = \frac{kT}{q} \ln\left(\frac{AA^*T^2}{I_o}\right)$$ (6.6)

When the applied voltage is sufficiently large enough, the effect of series resistance R_S is observed clearly on the curved section in the plots, (Figures 6.1 to 6.5) (Ozaydin and Akkilic, 2014, Schroder, 2015).

In this work, all obtained results from I-V data for reference diodes and with organic thin film diodes are summarized in (Table 6.1). The highest value of Φ_b are observed with (Sn) metal top contact, and the lowest one is with (Ni) metal without Phenol Red layer for reference contacts. The highest value of Φ_b with phenol red PSP interlayer is with (Sn) metal and lowest one is with (Ni) metal. From the values of

calculated barrier height for all the diodes, it can be noticed that the organic thin film increases barrier height Φ_b value for each sample with different top contact top contact metal.

Ideality factor values are varied from 1.289 to 5.459 for the reference devices, and for the devices with PSP layers are varied in the range of 1.108 to 1.833 (Table 6.1). Theoretically, ideality factor n equals to 1, for ideal diode, but ideality factor values of studied diodes was greater than 1. It is means that this increasement in n value can be related to the existence of interface layer, inhomogeneity in profiling barrier, the effect of image-force, tunneling effect, and recombination-generation process at interface (Ozaydin and Akkilic, 2014).

Table 6.1. Summary of rectification ratio R and electrical parameters R, n and Φ_b of M/p-Si diodes with and without PSP layer, where M = Ag, Cu, Ni, Pd and Sn from their I-V characteristics

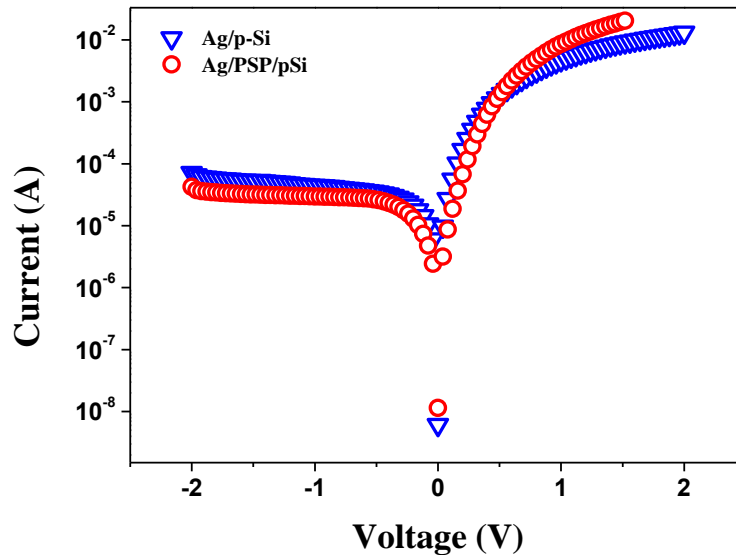| Metal	Φ_m (eV)	PSP	R	n	Φ_b (eV)	Ref	n	Φ_b (eV)
Ag	4.70		305.790	1.833	0.606		1.961	0.562
Cu	4.65		4870.16	1.146	0.687		1.289	0.558
Ni	5.15		3966.00	1.108	0.600		5.459	0.555
Pd	5.22		124818.8	1.272	0.724		2.802	0.648
Sn	5.40		7406.60	1.054	0.738		2.518	0.707

Figure 6.1. Experimental plots of *I-V* characteristics of Ag/p-Si and with PSP layer.

Figure 6.2. Experimental plots of *I-V* characteristics of Cu/p-Si and with PSP layer

.

Figure 6.3. Experimental plots of *I-V* characteristics of Ni/p-Si and with PSP layer.
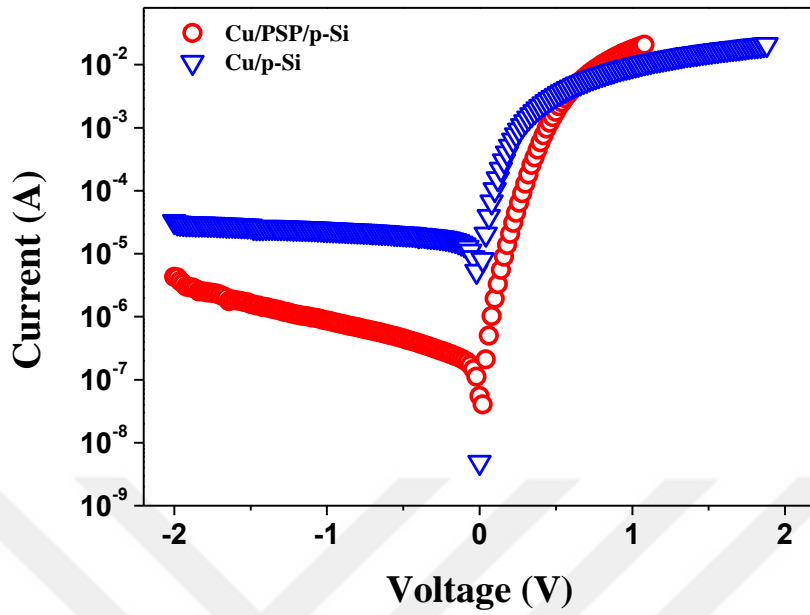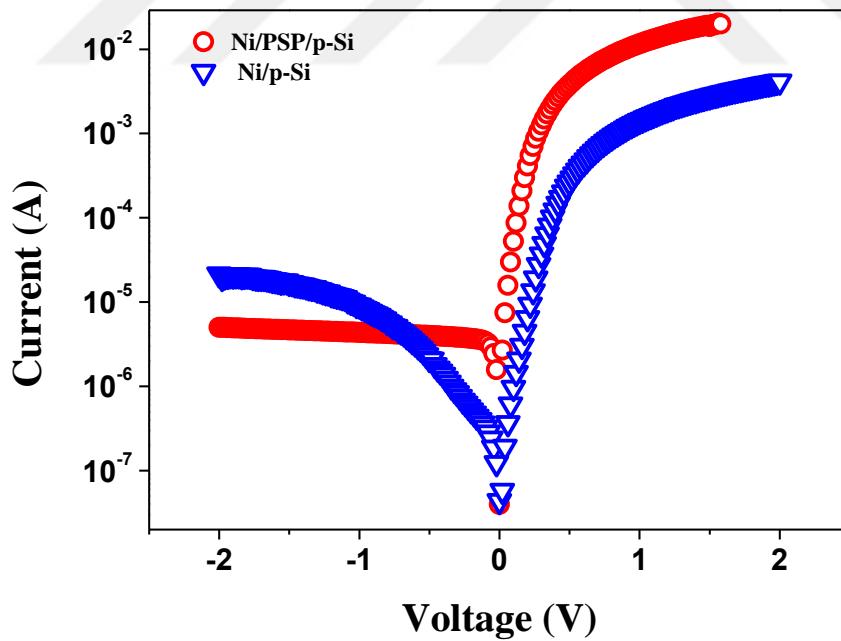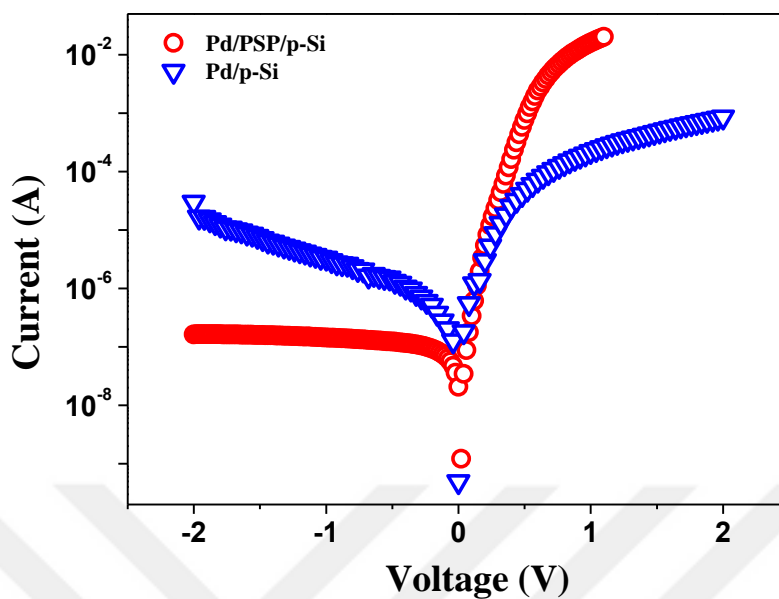
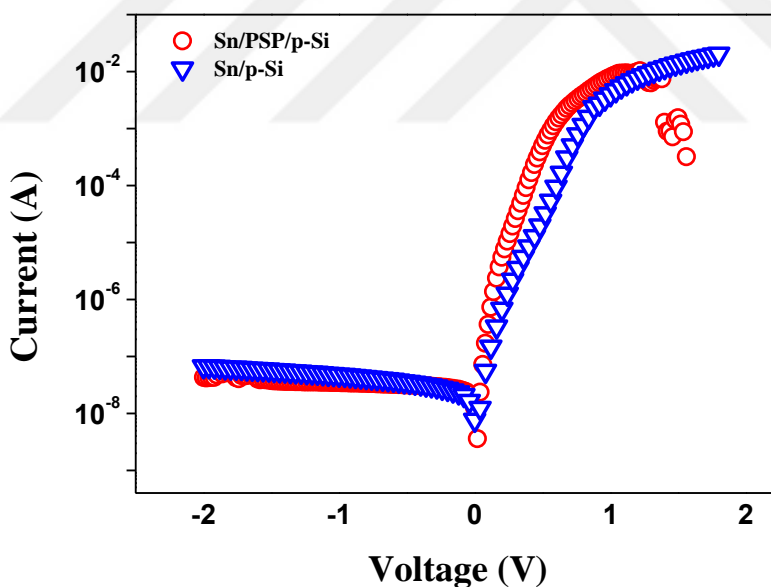Figure 6.4. Experimental plots of *I-V* characteristics of Pd/p-Si and with PSP layer.

Figure 6.5. Experimental plots of *I-V* characteristics of Sn/p-Si and with PSP layer.

In (figure 6.6) all different top contact metal *I-V* plots for metal/PSP/p-Si were represented, it is clearly observed the effect of metal work function on the devices which resulted different rectification ratio values of organic devices (Table 6.1).
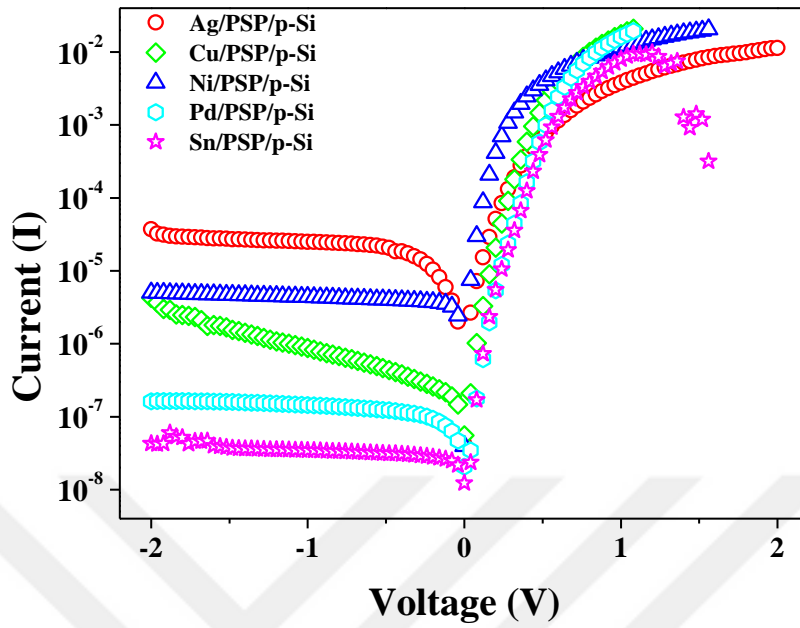
Figure 6.6. Experimental plots of *I-V* characteristics of M/PSP/p-Si, M = Ag, Cu, Ni, Pd and Sn.

6.2.1. Cheung I and CheungII calculation method.

In this calculation method, which introduced by Cheung and Cheung in 1986, the ideality factor value can be determined from linear section of current-voltage characteristics of diodes plot, when the applied voltage value is more than the amount of 3kT/q, and the role of resistance is notable, through given Eq

$$n = \frac{q}{kT} \frac{dV}{d\ln(I)} \tag{6.8}$$

Using this method, the obtained values of metal/PSP/p-Si diodes are more than unity. This difference could be as a result of interface charge density and series resistance effects (Benhaliliba et al, 2014).

When the applied voltage value is more than 3 kT/q, the effect of the resistance is noticable. In the plot of $\frac{dV}{d\ln I}$ versus I were taken, the intercept of this line with the y-axis is determined as *nkT/q,* and the slope of linear part plot gives R_s value using the following Eq.

$$\frac{dV}{d\ln I} = IR_s + n\left(\frac{kT}{q}\right) \tag{6.9}$$

Using a linear fit of the curves in the (Figures 6.7 to 6.11), and applying to Eq (6.8), (6.9), the electrical parameters n and R_s were calculated, the obtained results for these parameters form this method are inserted in (Table 6.2).

In Cheung II calculation, form the forward bias *I-V* data, H(I) function is estimated as in given Eq.

$$H(I) = V - \left(\frac{nkT}{q}\right)\ln\left(\frac{I}{AA^*T^2}\right) \tag{6.10}$$

When the *H* (I) curves exhibit a linear variation as function of current, as given in Eq.

$$H(I) = n\Phi_b + IR_s \tag{6.11}$$

From the linear fit of H(*I*) vs *I* lines in (Figures 6.7 to 6.11), the interception and slope of these lines gives $n\Phi_b$, and R_s, respectively. Thes parameters Φ_b and R_s obtained from the H(*I*) function are listed in (Table 6.2) (Selçuk et al, 2014, Benhaliliba et al, 2014).

Table 6.2. Electrical parameters summary from ChI-ChII characteristics of M/p-Si and M/PSP/p-Si where M = Ag, Cu, Ni, Pd and Sn

		dV/dln(*I*)		H(*I*)			dV/dln(*I*)		H(*I*)	
Metal	PSP	n	Rs (Ω)	Φ_b (eV)	Rs (Ω)	Ref	n	Rs (Ω)	Φ_b (eV)	Rs (Ω)
Ag		3.114	65.137	0.566	64.78		2.936	141.76	0.531	142.77
Cu		2.250	29.600	0.688	25.55		1.896	75.490	0.529	76.30
Ni		1.595	62.260	0.606	58.20		3.244	308.44	0.590	311.22
Pd		2.197	22.313	0.665	21.26		3.990	1988.2	0.610	1988.6
Sn		2.294	48.400	0.695	51.50		2.682	41.109	0.649	40.100

The values of R_s determined by the Equ (6.9) and (6.11) are almost similar. The R_s values of the devices without PSP are greater than those one of the samples with PSP layer. The ideality factor value was more than unity, were the values of ideality factors of prepared samples with organic layer are found to be in the range of 1.5 to 3. This is due to the existence of organic interfacial layer and series resistance (Chankaya and Ucar, 2004, Selçuk et al, 2014). The values of barrier height of the devices with PSP

layer are greater than that of devices without PSP layer. The values was 0.566 eV for Ag top contact metal and increases up to 0.695 eV for Sn top contact metal.
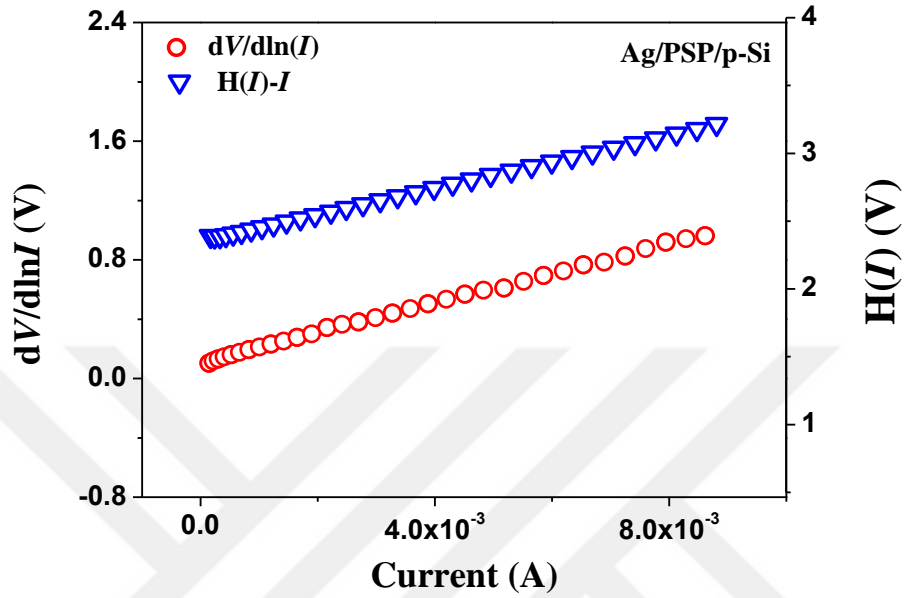

Figure 6.7. Plots of dV/dln(I) vs I with H(I) vs I characteristics of Ag/ PSP/p-Si hybrid structure.

.

Figure 6.8. Plots of dV/dln(I) vs I with H(I) vs I characteristics of Cu/ PSP/p-Si hybrid structure.

Figure 6.9. Plots of dV/dln(I) vs I with H(I) vs I characteristics of Ni/ PSP/p-Si hybrid structure.
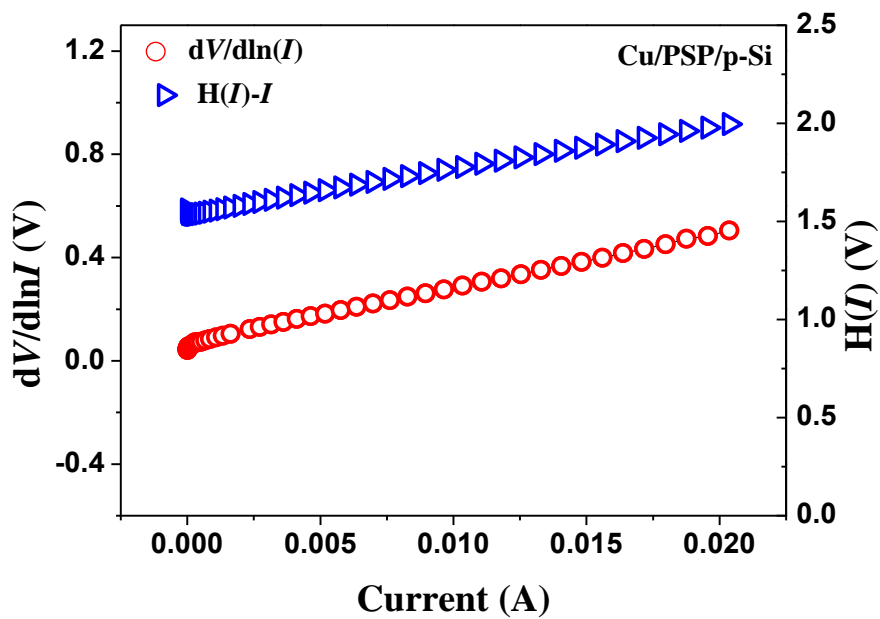

Figure 6.10. Plots of dV/dln(I) vs I with H(I) vs I of characteristics Pd/PSP/p-Si hybrid structure.

Figure 6.11. Plots of dV/dln(I) vs I with H(I) vs I characteristics of Sn/ PSP/p-Si hybrid structure.

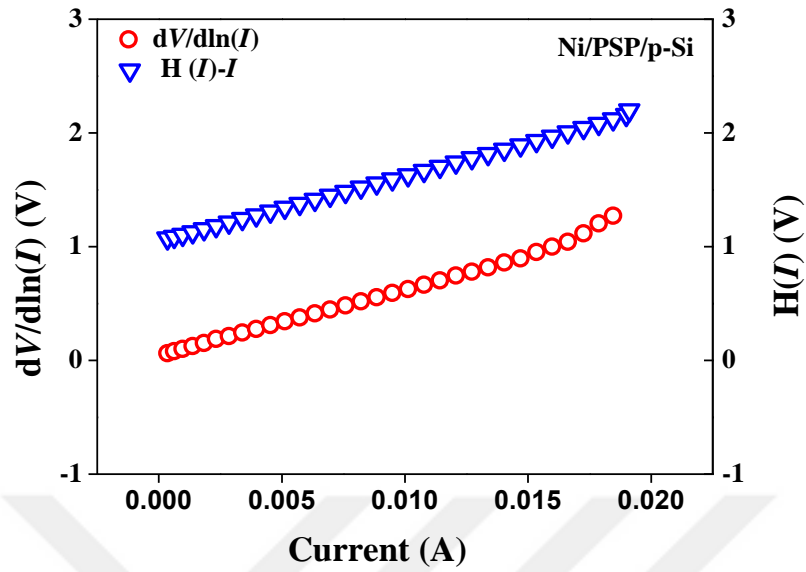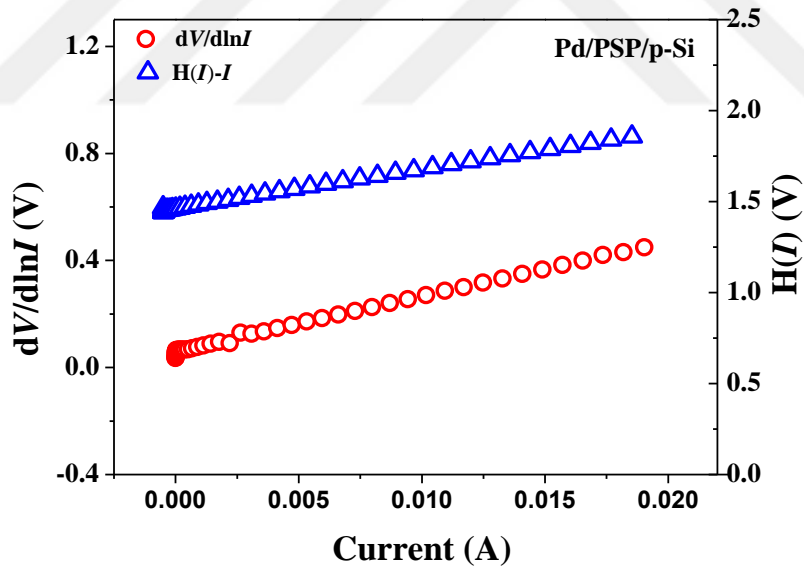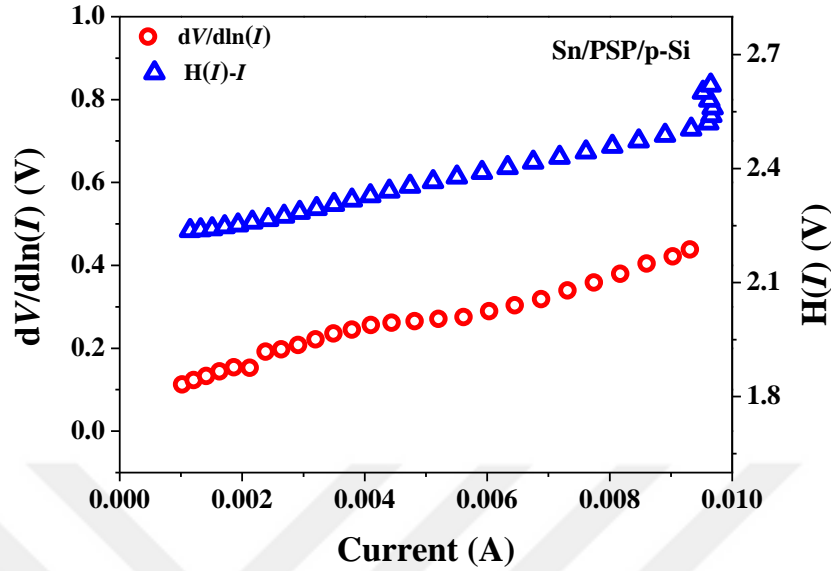## 6.2.2. Norde calculation method

To determine R_s and Φ_b ,an alternative method which was proposed by Norde (Norde, 1979), is Norde $F(V)$ function.

$$F(V) = \frac{V}{\gamma} - \frac{kT}{q} \ln\left(\frac{I(V)}{AA^*T^2}\right) \tag{6.12}$$

Where γ is the smallest integer number greater than n. By substituting forward bias I-V data, and n value obtained from *I-V* plot in Eq, F(V) vs V of graphs for the studied devices were plotted (Figures 6.12 to 6.16). After that, the minimum of the $F(V)$ function, an associated voltage (Vmin), and a related current (Imin) were determined to replace in following Eqs (6.13) and (6.14) for obtaining the R_s and Φ_b values (Benhaliliba et al, 2014, Tascioglu et al, 2013).

$$R_s = \frac{kT(\gamma - n)}{qI_{min}} \tag{6.13}$$

$$\Phi_b = F(V_{min}) + \frac{F(V\min)}{\gamma} - \frac{kT}{q} \tag{6.14}$$

The R_s values, calculated with this method are found to be in the range of 110.8 Ω to 4444 Ω for organic devices. The values of Φ_b for reference diodes and with organic interfacial layer diodes were obtained via Eq. (6.14), are presented in (Table 6.3). It is clearly observed that the values of Φ_b for the device with organic interlayer was higher than the values of diodes without organic interlayer for all metal top contacts.

Table 6.3. Summary of electrical parameters R_s, n and Φ_b of M/p-Si diodes with and without PSP layer, where M = Ag, Cu, Ni, Pd and Sn from modified Norde function

Metal	PSP	Φ_b (eV)	R_s	Ref	Φ_b (eV)	R_s
Ag		0.625	333.78		0.574	37.250
Cu		0.754	713.60		0.569	118.56
Ni		0.613	110.80		0.598	59.427
Pd		0.756	2271.0		0.717	7841.0
Sn		0.747	4444.0		0.746	5686.0

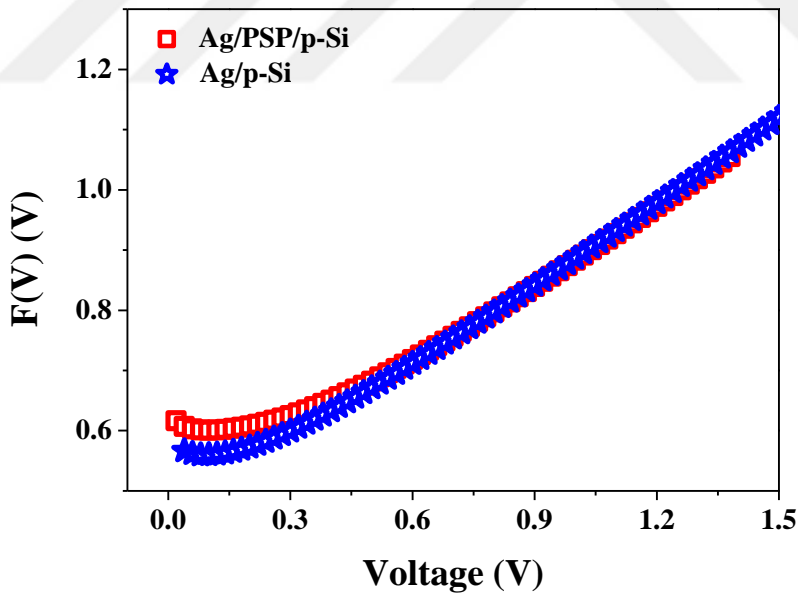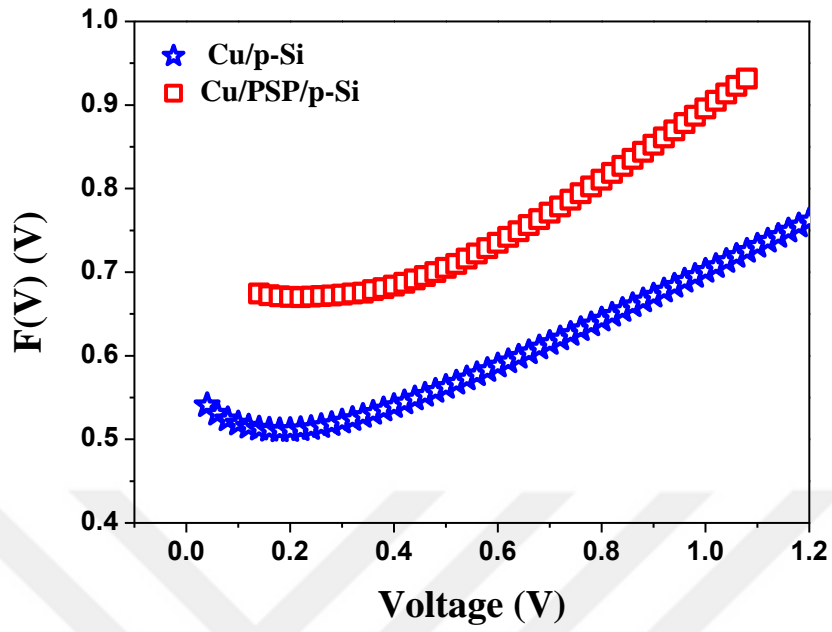Figure (6.12). F(V) vs V plots of Ag/p-Si and Ag/PSP/p-Si hybrid structure.

Figure (6.13). F(V) vs V plots of Cu/p-Si and Cu/PSP/p-Si hybrid structure.
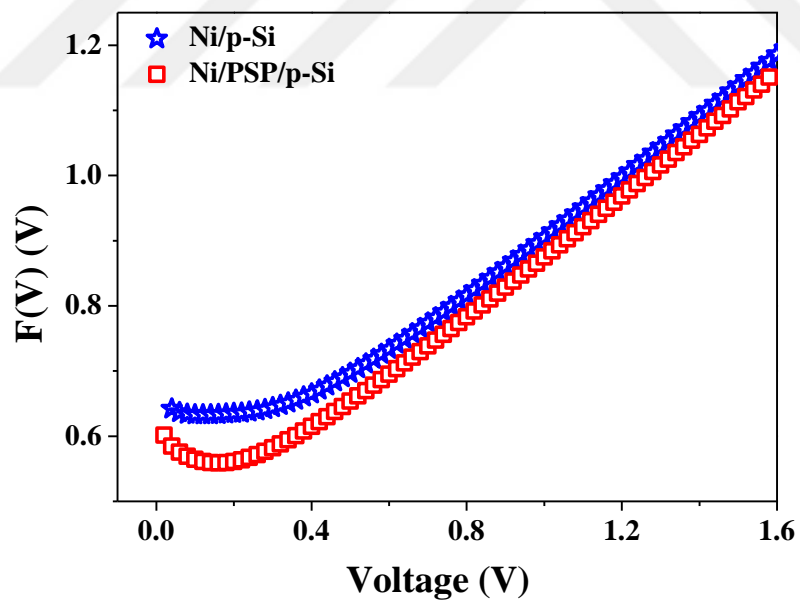

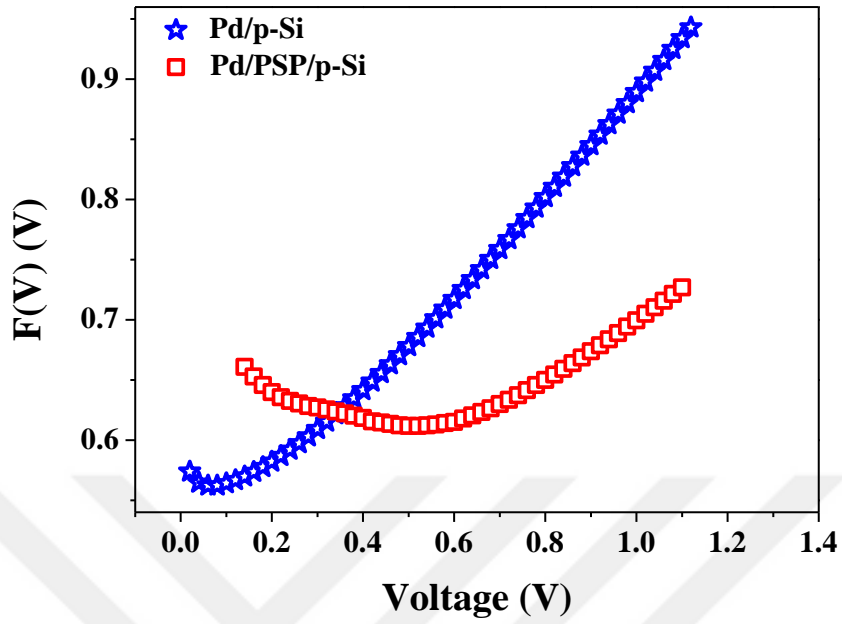Figure (6.14). F(V) vs V plots of Ni/p-Si and Ni/PSP/p-Si hybrid structure.

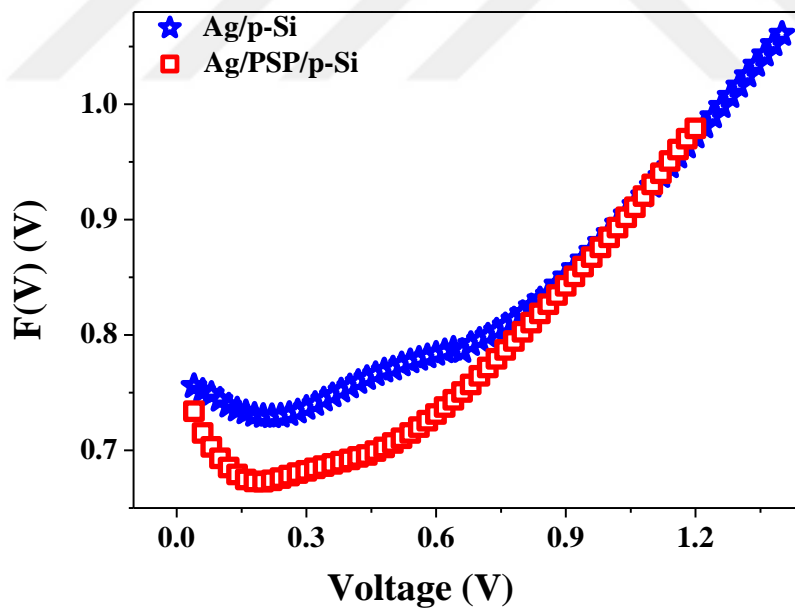Figure (6.15). *F*(V) vs *V* plots of Pd/p-Si and Pd/PSP/p-Si hybrid structure.

Figure 6.16. *F*(V) vs *V* plot of Sn/p-Si and Sn/PSP/p-Si hybrid structure.

6.3. Capacitance-Voltage Properties of Devices

Capacitance-voltage curves are another way to determine the main parameters, such as built in potential, Fermi energy, uncompensated acceptors concentration and barrier height of devices. The *C-V* relation in the reverse-biased region for Schottky barrier is given by

$$\frac{1}{C^2} = \frac{2(V_{bi} + V)}{q\varepsilon_s\varepsilon_o A^2 N_a} \tag{6.15}$$

$$\frac{\partial(1/C^2)}{\partial V} = \frac{2}{A^2\varepsilon_s\varepsilon_o q N_a} \tag{6.16}$$

The $1/C^{-2}$ versus applied voltage plot is linear at small voltage region. The slope of this line is used to obtain the doping level of the semiconductor via Eq (6.16). The built-in voltage (V_{bi}) equals to the voltage-axis intersection of this line (Kudryk et al, 2014, Parlaktürk et al, 2007).

$$V_{bi} = V_d - kT/q \tag{6.17}$$

where diffusion potential at zero bias is V_d, and Φ_b value can be obtained by *C-V* plot as in given equation

$$\Phi_b(C - V) = V_{bi} + E_F \tag{6.18}$$

where E_F is the Fermi energy, expressed as

$$E_F = \frac{k_B T}{q} \ln\left(\frac{N_a}{N_V}\right) \tag{6.19}$$

Schottky diode capacitance is used to determine the depletion layer width. This width is proportional with the applied voltage biasing according to following relation.

$$W \propto (V_{bi} \pm V)^{1/2} \tag{6.20}$$

Here in forward and reverse bias are represented by plus and minus signs, respectively. In the case of zerobias the width of depletion layer can be determined by given Eq.

$$W_d = \sqrt{\frac{2\varepsilon_s V_{bi}}{qN_a}} \tag{6.21}$$

The experimental *C-V* data was measured for metal/p-Si and metal/PSP/p-Si devices starting with applying frequency between 235 kHz upto 1.5 MHz as a function of voltage. The *C-V* plots of the samples are shown in (Figures 6.17-6.26). It is seen from the figures that the capacitance of devices depends on not only the applied bias voltage, but also the frequency. The C value decreases with the increasing frequency. This decrasing in C value is related to the insensitivity of interface charges to follow with AC signal (Sze, 1981). Furthermore, the voltage dependency on capacitance is so weak at the reverse bias regime comparing with the forward bias regime.

The experimental results reveals that the capacitance *C* of the diodes is a function of bias voltage and frequency particularly in accumulation zone, and the absolute value of capacitance *C* increases with decreasing the frequency in forward bias region (Korucu et al, 2013, Selçuk, 2014).

Abnormal peak is observed in plots of some devices plots under various frequencies. At low frequency, this peak shifts toward positive values of the voltage in (Figures 6.19 and 6.22). When the frequency is increased, the irregular peaks deviates towards positive values of high voltage in (Figures 6.17, 6.23 and 6.25). There is obvious effect of series resistance R_s at high frequencies on capacitance (Bilkan et al, 2015). Under various frequencies, at low frequency, this peaks shifts toward positive values of the voltage in (Figures 6.19 and 6.22). When the frequency is increased, the irregular peaks deviates towards positive values of high voltage in (Figures 6.17, 6.23 and 6.25). There is obvious effect of series resistance R_s at high frequencies on capacitance (Bilkan et al, 2015).

In Figures 6.22 and 6.24, it can be seen that, with increasing frequency values the capacity of device reduces. This may be due to the high-frequency insensitivity of the interface states to AC signal tracking. On the other hand, there is a significant impact of interface states charges on the capacitance characteristics of the devices.

Furthermore, it was observed a negative behavior of capacitance NC for Ni samples with PSP layer at high frequencies in forward bias of the plot, (Figure 6.22). The negative capacitance can be due to the presence of several reasons, such as

including series resistance effect, presence of organic thin layer, and interface density distribution (Selçuk et al, 2014, Zeyrek, 2015).

Figure 6.17. The plots of capacitance *C* (F) vs voltage *V*(V) measured at different frequencies for Ag/p-Si structure.

Figure 6.18. The plots of capacitance *C* (F) vs voltage *V*(V) measured at different frequencies for Ag/PSP/p-Si structure.
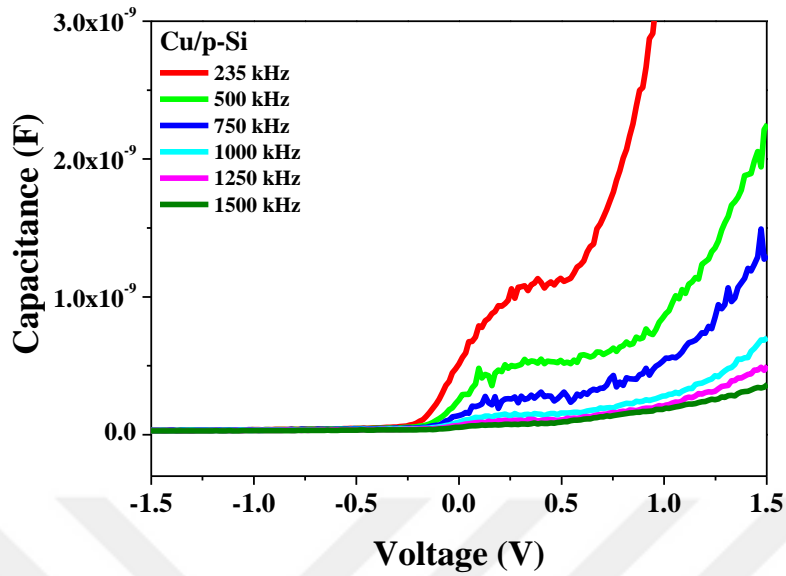
Figure 6.19. The plot of capacitance *C* (F) vs voltage *V*(V) measured at different frequencies for Cu/p-Si structure.
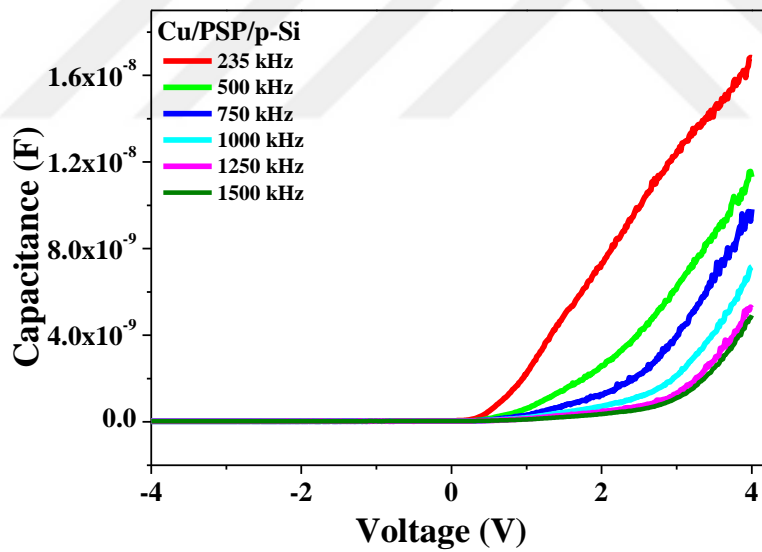
Figure 6.20. The plots of capacitance *C* (F) vs voltage *V*(V) measured at different frequencies for Cu/PSP/p-Si structure.
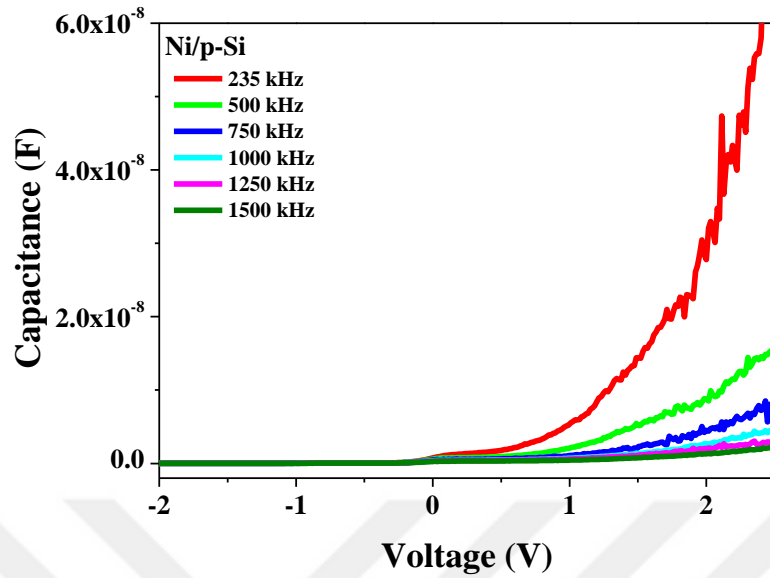
Figure 6.21. The plots of capacitance C (F) vs voltage V(V) measured at different frequencies for Ni/p-Si structure.

Figure 6.22. The plots of capacitance C (F) vs voltage V(V) measured at different frequencies for Ni/PSP/p-Si structure.

Figure 6.24. The plots of capacitance *C* (F) vs voltage *V*(V) measured at different frequencies for Pd/PSP/p-Si structure.
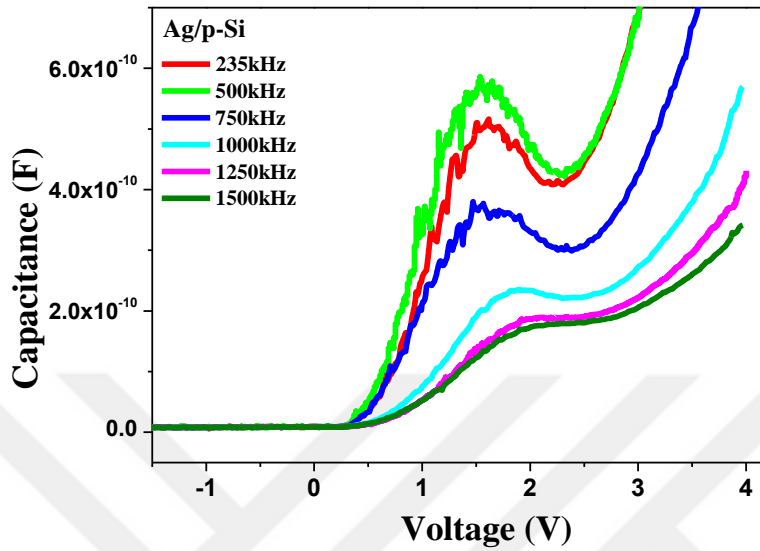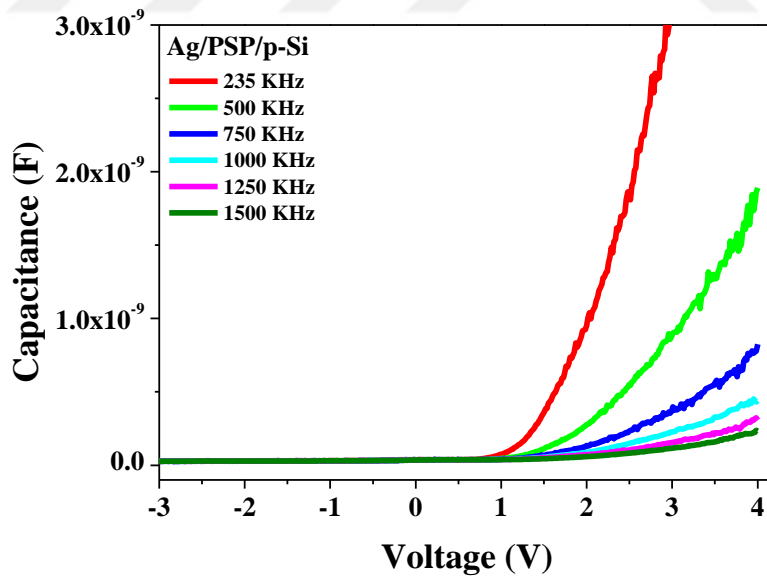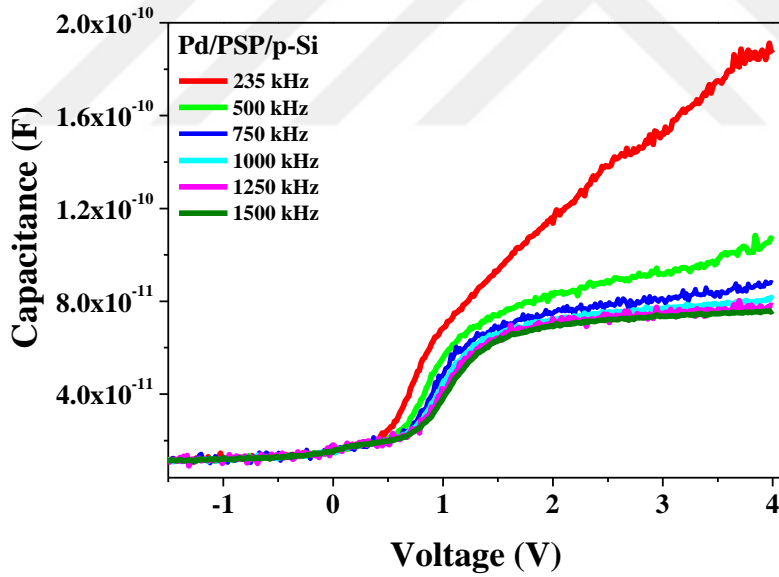

Figure 6.23. The plots of capacitance *C* (F) vs voltage *V*(V) measured at different frequencies for Pd/p-Si structure.
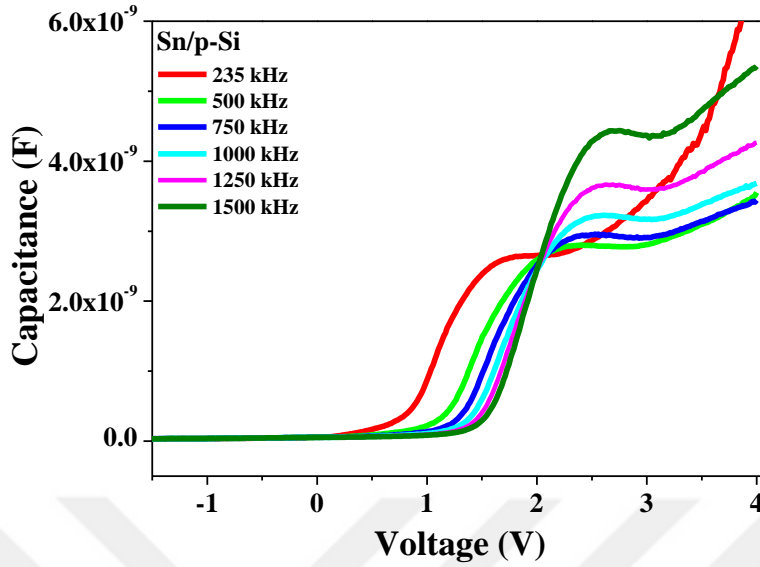
Figure 6.25. The plots of capacitance C (F) vs voltage V(V) measured at different frequencies for Sn/p-Si structure.
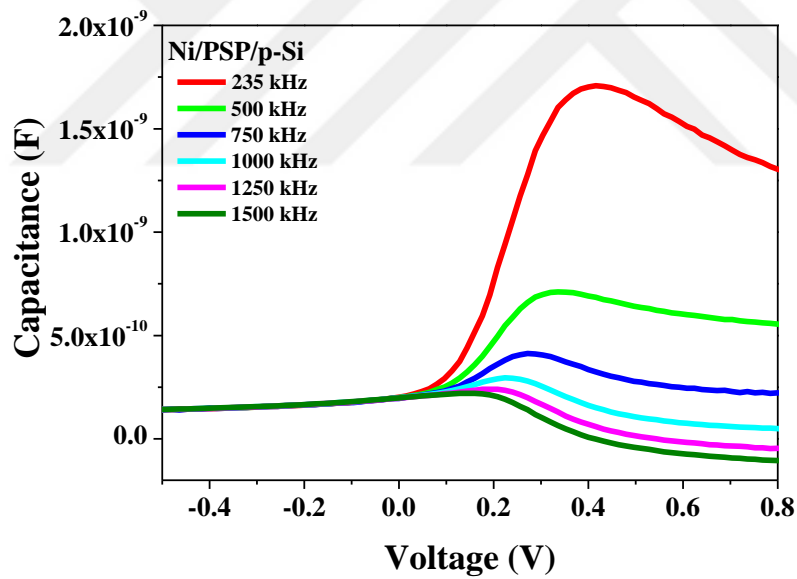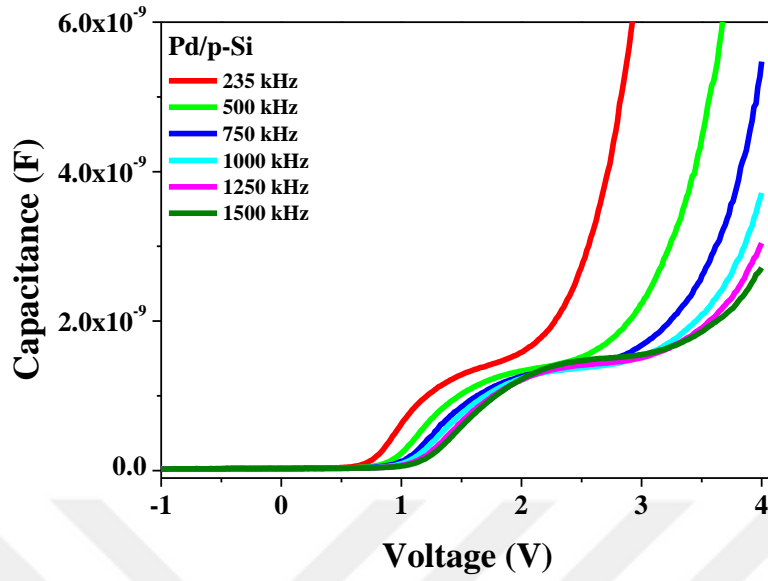
In C–V plot of (Figure 6.26), the values of capacitance increases when the applied forward bias voltage is increased, while the capacitance is approximately constant in the reverse bias of other frequencies. An excess capacitance phenomenon observed for the Sn/PSP/p-Si structure at low frequencies (235 kHz and 500 kHz). This related to the interface states charge capability at low frequency, and work function of Sn metal. In addition the highest capacitance value of the device dose not change dramatically, when the frequency is increases. It can be because of interface states insensitivity at the high frequency to follow the AC signal (Imer et al, 2016).

The C^{-2}–V curves for the reverse bias of the frequency value 235 kHz are plotted for metal/p-Si and metal/PSP/p-Si heterostructures, (Figures 6.21 to 6.25). From the linear part in depletion region of these plots, the slope of this linear part is identical with the localized doping concentration in a p-type semiconductor (Nicollian and Goetzberger, 1967).

From the results obtained from C^{-2} - V plots, barrier height values of the devices with PSP interfacial layer by using Eq (6.16). These values are higher than values of devices without organic interlayer. The presence of the organic thin films interlayer in the diodes can be the reason for this difference in results (Imer et al, 2015).
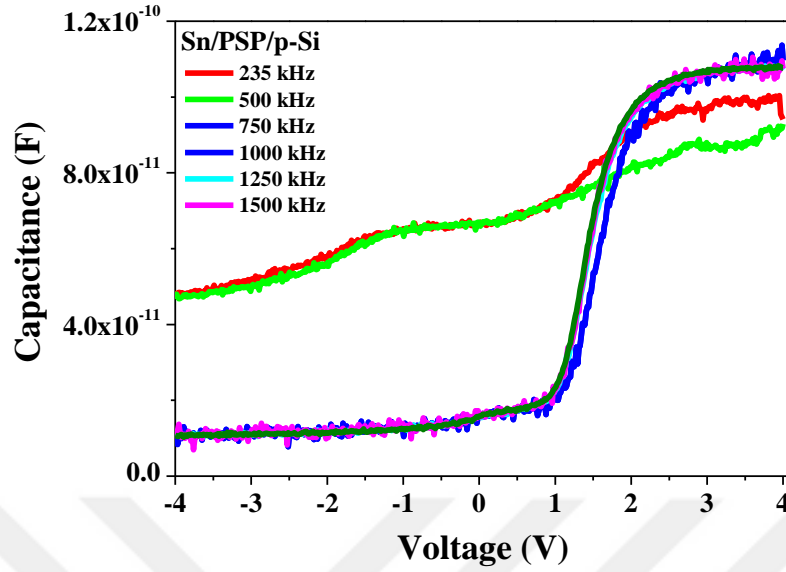
Figure 6.26. The capacitance C (F) vs voltage V(V) plot measured at different frequencies for Sn/PSP/p-Si structure.

The barrier height value of C^{-2}-V was also observed to be greater than the I-V results. These rise of barrier height values in C-V measurement corresponds to the results calculated from I-V data to the different nature of calculation methods namely Norde and CheungI-CheungII. The barrier height values for all diodes was between 0.622 eV to 0.948 eV. The highest value was with Sn top contact metal and the lowest one was with Cu top contact metal. In (Table 6.3), the obtained values of parameters E_F, V_{bi}, N_a, and Φ_b from (C^{-2}-V) are given.

Table 6.4. Summary of main electrical parameters of M/p-Si diodes with and without PSP layer, where M = (Ag, Cu, Ni, Pd and Sn) from their C^{-2}-V characteristics.

	M/ PSP/P-Si				M/P-Si			
Metal	Φ_b (eV)	Vbi (V)	Nd (cm^{-2})	Ef (eV)	Φ_b (eV)	Vbi(V)	Nd(cm^{-2})	Ef (eV)
Ag	0.921	0.715	3.553×10^{15}	0.207	0.685	0.426	4.579×10^{14}	0.260
Cu	0.626	0.444	9.069×10^{15}	0.182	0.569	0.326	8.604×10^{14}	0.243
Ni	0.796	0.600	5.320×10^{15}	0.196	0.691	0.447	8.312×10^{14}	0.244
Pd	0.821	0.621	4.677×10^{15}	0.199	0.682	0.447	1.170×10^{15}	0.235
Sn	0.948	0.774	1.220×10^{16}	0.175	0.822	0.575	7.332×10^{14}	0.247

Figure 6.27. The C^{-2} (F) vs V (V) curves of Ag/p-Si and with PSP interlayer structure.

Figure 6.28. The C^{-2} (F) vs V (V) curves of Cu/p-Si and with PSP interlayer structure.

Figure 6.29. The C^{-2} (F) vs V (V) curves of Ni/p-Si and with PSP interlayer structure.

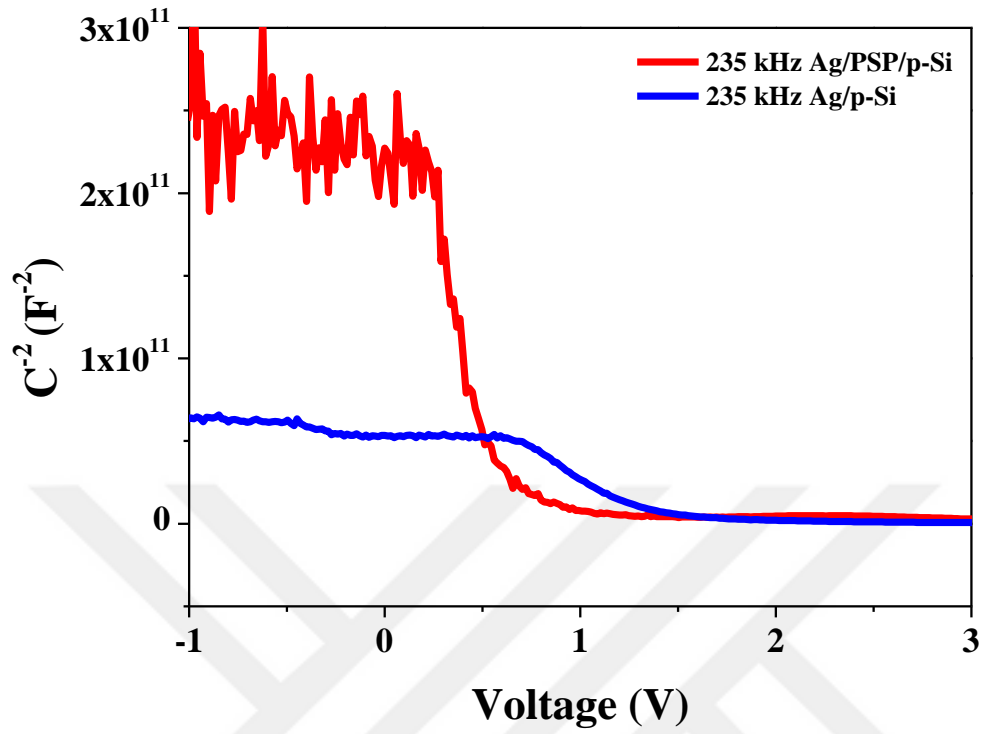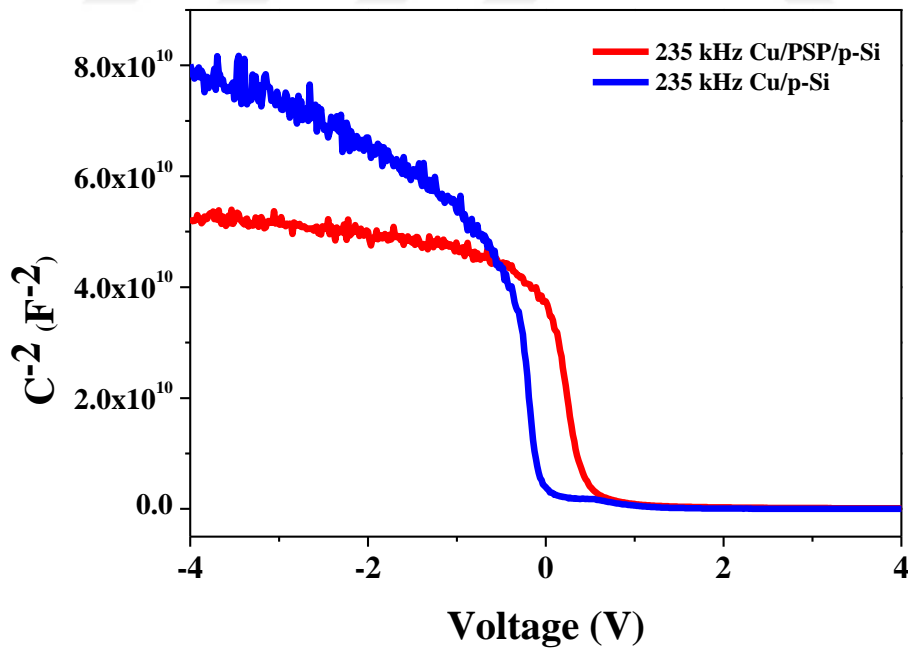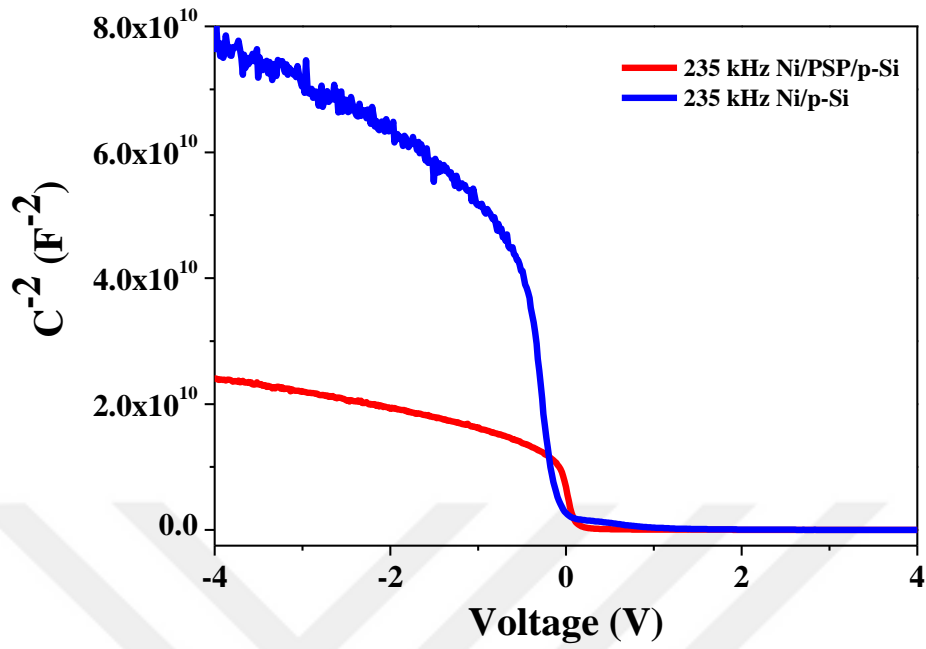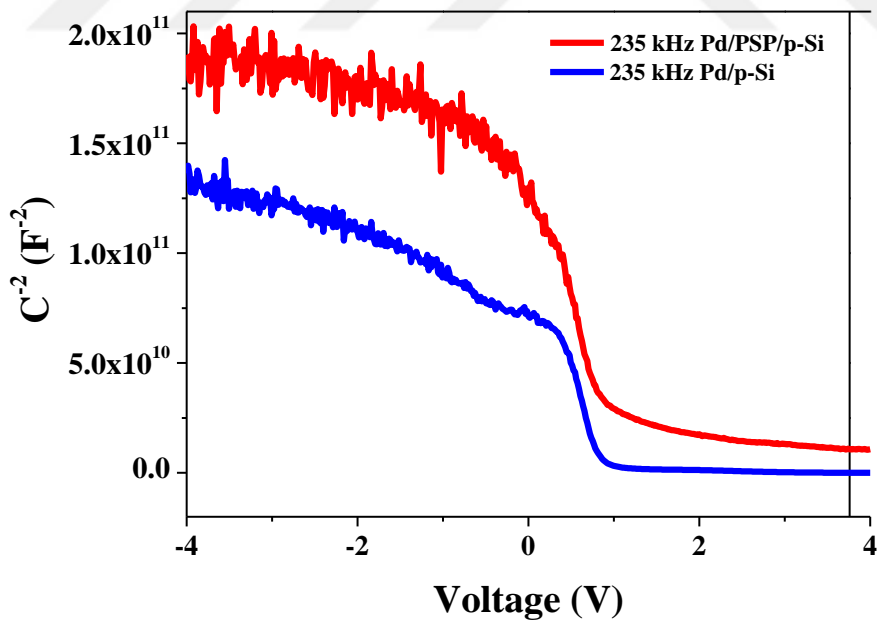Figure 6.30.The C^{-2} (F) vs V (V) curves of Pd/p-Si and with PSP interlayer structure.
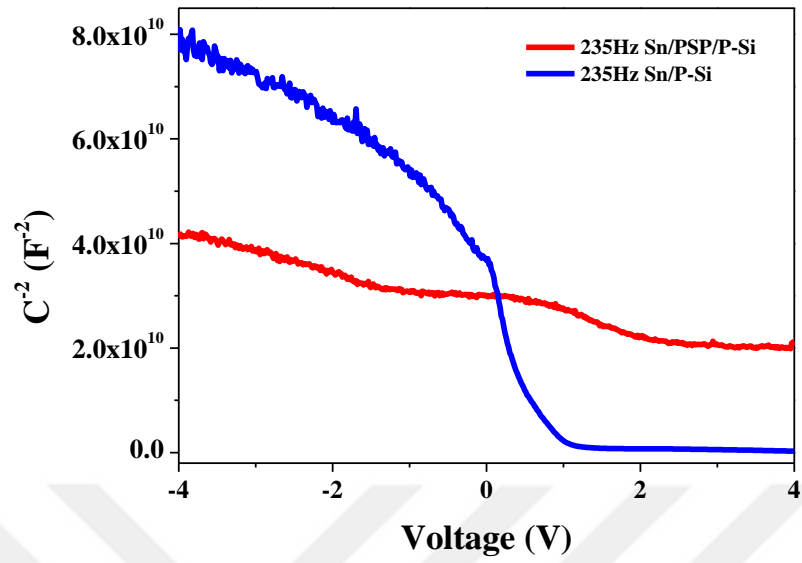
Figure 6.31. The C^{-2} (F) vs V (V) curves of Sn/p-Si and with PSP interlayer structure.

7. CONCLUSION

In this thesis, the effect of work function of metal and PSP interlayer on the electrical parameters of hybrid structure with different top contact metals were examined. The devices were fabricated by spin coating method to deposit a phenol red organic dye thin film as an interfacial layer between the semiconductor and metal top contacts. In addition, thermal evaporation method was used to deposit the different metal top contacts.

To investigate the results of the electrical parameters of fabricated diodes, different methods were used such as capacitance-voltage and current-voltage measurements, the clculation results are confirmed via Norde and Cheung I-II. The *I-V* plots and obtained results of the diodes with and without organic layer showed rectification behavior, (see Table 6.1). The results of calculated barrier height of organic based devices obtained from the different calculation methods were higher than the results of reference diodes. There was an agreement between the values from *I-V*, Norde and Cheung methods. These results are confirmed the possibility of the optimization in the electrical parameters of the devices. As a conclusion, the inserting of the organic interlayer modifies the electrical properties of the diodes, like decreasing the series resistance and increasing the barrier height of the devices. Therefore, fabricated devices with organic layer are good candidate for many electronic applications, such as rectifiers, electronic devices and sensors.

The barrier height value depends on the type of the contact metal work function and the used organic interlayer materials. Previous experimental studied shows that there is a possibility to change Schottky barrier height by adding organic materials. Obtained results in this study shows that the calculated barrier height values of diodes with organic layer increases comparing with diode without organic layer for every samples.

The Schottky diode parameters like ideality factor n and barrier height Φ_b, series resistance R_S were also calculated using CheungI-CheungII and Norde function. Applying to Cheung's and Norde calculation methods, there was a good

agreement in the obtained results of series resistance R_S from Cheung's calculation. Although, there was obvious difference in series resistance values calculated from Norde and Cheung's method.

A disparity was seen between values of the ideality factor n calculated with Norde and cheungI-II methods. This discrepancy in values can be due to the series resistance R_s effects. Possible reasons are to include interface states charges, Schottky barrier height Φ_b dependence on the bias voltage drops through the thin layer organic material, and low voltage in forward bias of the current-voltage plots. In all calculation methods, the obtained ideality factor results of prepared diodes are higher than the unity. .

From $C\text{-}V$ measurements, E_F, V_{bi}, N_a and Φ_b values were determined. The barrier height values calculated by $C\text{-}V$ method shows an agreement with that of other methods. The calculated barrier height from capacitance-voltage method was different, this is due to being frequency dependent on capacitance-voltage property of the organic devices which investigated between 235 kHz to1.5 MHz frequencies. $C\text{-}V$ plots of devices in both biasing shows that the behavior of capacitance can be due to interface state distribution, and series resistance R_s effect.

Extra examination of the electrical parameters of devices was performed. The $C\text{–}V$ measurements of forward and reverse bias voltage under different frequencies are done for the diodes. The capacitance values of devices are enhanced with increasing in applied forward voltage. Conversly, it was almost constant for the reverse bias voltage regime. The capacitance value of the devices decreases when the frequency increases. This is probably caused by the interface states insensitivity to follow the AC signal at the greater frequency values.

As seen from results of devices electrical parameters obtained from different measurements, a relative difference can be seen between values of electrical parameters Φ_b, n and R_s of the diodes. This difference can be attributed to the normal nature of I-V and C-V measurement techniques.

REFERENCES

Ahmad, Z., Sayyad, M. H., 2008. Investigation of the electronic Properties of Au/methyl-red/Ag surface type Schottky diode by current-voltage method. *Chapter 8 Ag/OD-MO/Ag Surface-type Diode Proc. World Academy of Science, Engineering and Technology* :588-590.

Akkaya, A., 2018. The current–voltage and capacitance–voltage characterization of the Au/Methylene Blue/n-GaAs organic-modified Schottky diodes. *Anadolu Üniversitesi Bilim Ve Teknoloji Dergisi A-Uygulamalı Bilimler ve Mühendislik*, **19**(3): 756-767.

Al Orainy, R. H., 2014. Electrical characterization of a Schottky diode based on organic semiconductor film. *Journal of Optoelectronics and Advanced Materials*, **16** (7-8): 793-797.

AL-Ghamdi, S., 2009. *Study Of Some Physical Properties Of Organic Material Tetracyanoquinodimethane (TCNQ). (Master Thesis)*. Girls – faculty of education scientific departments, King Abdulaziz univarsity , Jeedah.

Al-Ta'ii, H., Periasamy, V., Amin, Y., 2015. Electronic properties of DNA-based Schottky barrier diodes in response to alpha particles. *Sensors*, **15**(5): 11836-11853.

Ayala, K., 2013. *Study of Charge Carrier Transport in Organic Semiconductors* (Ph.D Thesis). Instituto Nacional de Astrof´ısica, O´ ptica y Electro´nica, Tonantzintla, Puebla.

Aydin, M. E., Yakuphanoglu, F., 2007. Molecular control over Ag/p-Si diode by organic layer. *Journal of Physics and Chemistry of Solids*, **68**(9): 1770-1773.

Basman, N., 2017. Effect of a new methacrylic monomer on diode parameters of Ag/p-Si Schottky contact. *Informacije MIDEM*, **46**(4): 190-196.

Basman, N., 2017. Effect of a new methacrylic monomer on diode parameters of Ag/p-Si Schottky contact. *Informacije MIDEM*, **46**(4): 190-196.

Bässler, H., Köhler, A., 2011. Charge transport in organic semiconductors. *Unimolecular and Supramolecular Electronics I* (1-65).

Benhaliliba, M., Ocak, Y. S., Benouis, C. E., 2014. Effect of metal on characteristics of MPc organic diodes. *Журнал Нано-Та Електронної Фізики*, **6**(4): 04009-1.

Bilkan, Ç., Gümüş, A., Altındal, Ş., 2015. The source of negative capacitance and anomalous peak in the forward bias capacitance-voltage in Cr/p-si Schottky barrier diodes (SBDs). *Materials Science in Semiconductor Processing*, **39**: 484-491.

Bohlin, K. E., 1986. Generalized norde plot including determination of the ideality factor. *Journal of Applied Physics*, **60**(3): 1223-1224.

Bozhkov, V. G., Torkhov, N. A., Shmargunov, A.V., 2011. About the determination of the Schottky barrier height with the CV method. *Journal of Applied Physics*, **109**(7): 073714

Braun, S., 2007. *Studies Of Materials and İnterfaces For Organic Electronics* (Doctoral dissertation), Institutionen för fysik, kemi och biologi). Linkoping, Sweden.

Brédas, J. L., Calbert, J. P., da Silva Filho, D. A., Cornil, J., 2002. Organic semiconductors: A theoretical characterization of the basic parameters governing

charge transport. *Proceedings of The National Academy Of Sciences*, **99**(9): 5804-5809.

Brütting, W,. 2005. *Physics of Organic Semiconductors(7B)From pdf.drive*

Carey, F. A., Sundberg, R. J., 2007. *Advanced Organic Chemistry: part* A: structure and mechanisms. Springer science and business media,university of Virginia. (fifth edition)

Colinge, J. P., Colinge, C. A., 2005. *Physics Of Semiconductor Devices*. Springer science and business media.

Coropceanu, V., Cornil, J., da Silva Filho, D. A., Olivier, Y., Silbey, R., Brédas, J. L., 2007. Charge transport in organic semiconductors. *Chemical Reviews*, **107**(4): 926-952.

Çankaya, G., Ucar, N., 2004. Schottky barrier height dependence on the metal work function for p-type Si Schottky diodes. *Zeitschrift Für Naturforschung A*, **59**(11): 795-798.

Dey, A., Singh, A., Das, D., Iyer, P. K., 2015. Organic semiconductors: a new future of nanodevices and applications. *Thin Film Structures in Energy Applications* (97-128).

Donchev, E., 2015. *Thin-Film Diode Structures For Advanced Energy Applications.* (Doctoral dissertation), Imperial College, London.

Gromov, D., Pugachevich, V., 1994. Modified methods for the calculation of real Schottky-diode parameters. *Applied Physics A*, **59**(3): 331-333.

Güllü, Ö., 2016. Barrier modification by methyl violet organic dye molecules of Ag/P-InP structures. *European Journal of Interdisciplinary Studies*, **2**(3): 7-17.

Güllü, Ö., Aydoğan, Ş., Türüt, A., 2012. High barrier Schottky diode with organic interlayer. *Solid State Communications,* **152**(5): 381-385.

Güllü, Ö., Kilicoglu, T., Türüt, A., 2010. Electronic properties of the metal/organic interlayer/inorganic semiconductor sandwich device. *Journal of Physics and Chemistry of Solids*, **71**(3): 351-356.

Güllü, Ö., Türüt, A., 2009. Electrical analysis of organic interlayer based metal/interlayer/semiconductor diode structures. *Journal of Applied Physics*, **106**(10): 103717

Güllü, Ö., Türüt, A., 2010. Electrical analysis of organic dye-based MIS Schottky contacts. *Microelectronic Engineering*, **87**(12): 2482-2487.

Güllü, Ö., Türüt, A., 2015. Electronic parameters of MIS Schottky diodes with DNA biopolymer interlayer. *Materials Science-Poland*, **33**(3): 593-600.

Imer, A. G., Karaduman, O., Yakuphanoglu, F., 2016. Controlling of the photosensing properties of Al/DMY/p-Si heterojunctions by the interface layer thickness. *Synthetic Metals*, **221** :114-119.

IMER, A. G., TOMBAK, A., KORKUT, A., 2017. Effect of ıllumination on the photovoltaic parameters of Al/p-Si Diode with an organic ınterlayer prepared by spin coating method. *Süleyman Demirel Üniversitesi Fen Bilimleri Enstitüsü Dergisi*, **21**(1): 153-157.

Janardhanam, V., Yun, H. J., Jyothi, I., Lee, J., Hong, H., Reddy, V. R., Choi, C. J., 2015. Energy-level alignment and electrical properties of Al/p-type Si Schottky diodes with sorbitol-doped PEDOT: PSS as an organic interlayer. *Journal of Alloys and Compounds*, **637**: 84-89.

Karadeniz, S., Barış, B., Yüksel, Ö.F., Tuğluoğlu, N., 2013. Analysis of electrical properties of Al/p-Si Schottky contacts with and without rubrene layer. *Synthetic Metals*, **168**: 16-22.

Kırsoy, A., Ahmetoglu, M., Asimov, A., Kucur, B., 2015. The electrical properties of Au/P3HT/n-GaAs Schottky barrier diode. *Acta Physica Polonica A*, 128 (2B).

Kim, K. D., Koo, J. B., Lee, J. K., Yang, Y. S., You, I. K., Noh, Y. Y., 2010. Variations in the electric characteristics of an organic schottky diode with the P3HT thickness. *Journal Of The Korean Physical Society*, **57**(1): 124-127.

Korucu, D., Turut, A., Altındal, Ş., 2013. The origin of negative capacitance in Au/n-GaAs Schottky barrier diodes (SBDs) prepared by photolithography technique in the wide frequency range. *Current Applied Physics*, **13**(6): 1101-1108.

Kudryk, Y. Y., Shynkarenko, V. V., Slipokurov, V. S., Bigun, R. I., Kudryk, R. Y., 2014. Determination of the Schottky barrier height in diodes based on Au–TiB–n-SiC 6H from the current-voltage and capacitance-voltage characteristics. *Semiconductor Physics Quantum Electronics and Optoelectronics,* **17**(4): 398-402.

Lee, T. C., Fung, S., Beling, C. D., Au, H. L., 1992. A systematic approach to the measurement of ideality factor, series resistance, and barrier height for Schottky diodes. *Journal of applied physics*, **72**(10): 4739-4742.

Lien, C. D., So, F. C. T., Nicolet, M. A., 1984. An improved forward IV method for nonideal Schottky diodes with high series resistance. *IEEE Transactions on Electron Devices*, **31**(10): 1502-1503.

Manikandan, N., Shanthi, B., Muruganand, S., 2015. Construction of spin coating machine controlled by arm processor for physical studies of PVA. *International Journal of Electronics and Electrical Engineering*, **3**(4): 318-322.

Mishra, U., Singh, J., 2007. *Semiconductor Device Physics and Design*. Springer science and business media.

Mohamad, K. A., Hoh, H. T., Alias, A., Ghosh, B. K. , Fukuda, H., 2017. Frequency and voltage dependent electrical responses of poly (triarylamine) thin film-based organic Schottky diode. *In EPJ Web of Conferences*, **162**(01060): 050-8585.

Nassajy, A., 2015**.** *Optimization Of Organic Schottky Diode Contact By Electrochemical Treatment Of Electrodes* (Master's thesis), Faculty Of Computing And Electrical Engineering,Tampere unıversıty of technology.

Ng, K. K., 2002. *Complete Guide To Semiconductor Devices* :431-437.

Nicollian, E. H., Goetzberger, A., 1967. The si-sio, interface–electrical properties as determined by the metal-insulator-silicon conductance technique. *The Bell System Technical Journal*, **46**(6): 1055-1033.

Norde, H., 1979. A modified forward I- V plot for Schottky diodes with high series resistance. *Journal of Applied Physics*, **50**(7): 5052-5053.

Ozaydin, C., Akkilic, K., 2015. Electrical and photoelectrical properties of copper (II) complex/n-Si/Au heterojunction diode. *American Journal of Optics and Photonics*, **2**(6): 69-74.

Parlaktürk, F., Agasiev, A., Tataroğlu, A., Altindal, Ş., 2007. Current-Voltage (IV) and capacitance-voltage (CV) characteristics of Au/Bi4Ti3O12/SnO2 structures. *Gazi University Journal of Science*, **20**(4): 97-102.

Podzorov, V., Menard, E., Borissov, A., Kiryukhin, V., Rogers, J. A., Gershenson, M. E., 2004. Intrinsic charge transport on the surface of organic semiconductors. *Physical Review Letters*, **93**(8):

Radke, S., 2011. *Charge Transport in Organic Semiconductors* (Diploma Thesis). Technısche unıvesıtat, Dresden.

Reddy, P. S., Janardhanam, V., Jyothi, I., Yuk, S. H., Reddy, V. R., Jeong, J. C., Lee, S. N. , Choi, C. J., 2016. Modification of Schottky barrier properties of Ti/p-type InP Schottky diode by polyaniline (PANI) organic interlayer. *Journal Of Semıconductor Technology and Scıence*, **16**(5): 664-674.

Schroder, D.K., 2015. *Semiconductor Material and Device Characterization*. John Wiley and Sons. United states of America.

Selçuk, A. B., Ocak, S. B., Kahraman, G., Selcuk, A. H., 2014. Investigation of diode parameters using I–V and C–V characteristics of Al/maleic anhydride (MA)/p-Si structure. *Bulletin of Materials Science*, **37**(7): 1717-1724.

Shinar, R., Shinar, J., 2009. *Organic Electronics in Sensors and Biotechnology*. New York, NY, USA:: McGraw-Hill.

Shkir, M., Ganesh, V., AlFaify, S., Yahia, I. S., 2017. Structural, linear and third order nonlinear optical properties of drop casting deposited high quality nanocrystalline phenol red thin films. *Journal of Materials Science: Materials in Electronics*, **28**(14): 10573-10581.

Stella, M., 2009. Study of organic semiconductors for device application. (Doctora thesis). Department de fisica aplicada I optica, universitat De Barcelona.

Sze, S. M., 2008. *Semiconductor Devices: Physics and Technology*. John wiley and sons. Taiwan.

Sze, S. M., Ng, K. K., 2006. *Physics Of Semiconductor Devices*. John wiley and sons.

Taşçıoğlu, İ., Altındal, Ş., Polat, İ., Bacaksız, E., 2013. The effect of metal work function on the barrier height of metal/CdS/SnO2/In–Ga structures. *Current Applied Physics*, **13**(7):1306-1310.

Thorsmølle, V. K., Averitt, R. D., Demsar, J., Smith, D. L., Tretiak, S., Martin, R. L., Chi, X., Crone, B. K., Ramirez, A. P. Taylor, A. J., 2009. Morphology effectively controls singlet-triplet exciton relaxation and charge transport in organic semiconductors. *Physical Review Letters*, **102**(1): 017401

Valeev, E. F., Coropceanu, V., da Silva Filho, D. A., Salman, S., Brédas, J. L., 2006. Effect of electronic polarization on charge-transport parameters in molecular organic semiconductors. *Journal of the American Chemical Society*, **128**(30): 9882-9886.

Verma, S., Kabiraj, D., Kumar, T., Kumar, S., Kanjilal, D., 2011, July. Dependence of Schottky barrier height on metal work function. **In** *AIP Conference Proceedings,* **1349**(1): 1111-1112.

Waddell, T. G., 2003. *Advanced Organic Chemistry, Part B: Reactions and Synthesis*, (Sundberg, Richard J.; Carey, Francis A.).

Yakuphanoglu, F., 2008. Determination of electronic properties of Al/p-Si/composite organic semiconductor (MIOS) junction barrier by current–voltage and capacitance–voltage methods. *Synthetic Metals*, **158**(3-4): 108-112.

Yakuphanoglu, F., Kandaz, M., Senkal, B. F., 2008. Current–voltage and capacitance– voltage characteristics of Al/p-type silicon/organic semiconductor based on phthalocyanine rectifier contact. *Thin Solid Films*, **516**(23): 8793-8796.

Yakuphanoglu, F., Şenkal, B. F., 2007. Electronic and thermoelectric properties of polyaniline organic semiconductor and electrical characterization of Al/PANI MIS diode. *The Journal of Physical Chemistry C*, **111**(4): 1840-1846.

Yildiz, D. E., Apaydin, D. H., Kaya, E., Altindal, S., Cirpan, A., 2013. The main electrical and interfacial properties of benzotriazole and fluorene based organic devices. *Journal of Macromolecular Science, Part A*, **50**(2): 168-174.

Yüksel, Ö. F., Tuğluoğlu, N., Gülveren, B., Şafak, H., Kuş, M., 2013. Electrical properties of Au/perylene-monoimide/p-Si Schottky diode. *Journal of Alloys and Compounds*, **577**: 30-36.

ORGANİK BOYA TABANLI HİBRİT YAPININ ELEKTRİKSEL PARAMETRELERİNE METALİN İŞ FONKSİYONUNUN ETKİSİNİN İNCELENMESİ

OMARBLI, Sabiha Abdullah
Yüksek Lisans Tezi, Fizik Anabilim Dalı
Tez Danışmanı: Doç. Dr. Arife GENÇER İMER
Ocak, 2020, 79 Sayfa

ÖZET

Bu tez çalışmasında, fenol kirmizisi (PSP) bileşenli heteroeklem aygıtların elektronik parametreleri belirlenmiştir. Çalışmada, (100) yönelimine sahip ve özdirenci 1-10 Ω-cm olan p-Si yarıiletken kristali üzerine, metanolde çözülerek hazırlanmış $1x10^{-2}$ molarlık organik boyar çözelti dönel kaplama (spin coating) metoduyla ince organik arayüzey tabaka olarak kaplandı. Üst kontak yapmak için yüksek vakum ortamında 5 farklı metal (M;Ag, Cu, Ni, Pd, Sn) termal buharlaştırılarak M/PSP/p-Si/Al hibrit yapıları elde edilmiştir. Üretilen aygıtların elektriksel karakteristik özellikleri incelenip analiz edilmiştir.

Aygıtların elektriksel parametreleri oda sıcaklığında ve karanlık ortamda akım-gerilim (*I-V*) ve kapasite-gerilim (*C-V*) ölçümleri yardımıyla incelendi. Buna göre her aygıtta düz beslem *I-V* ölçümlerinden idealite faktörü, engel yüksekliği gibi elektrik parametreleri, logaritmik I-V, Cheung, ve Norde fonksiyonları yardımıyla hesaplandı. Tüm yöntemlerden elde edilen sonuçlar karşılaştırıldı, ve yorumlandı. Elde edilen tüm bulgulara dayanarak metalin iş fonksiyonun ve organik ara yüzeyin aygıtın elektriksel parametrelerine etkisi detaylı olarak incelendi. Aygıtın elektronik özelliklerinin organik film yardımıyla iyileştiği tespit edilmiştir.

Anahtar kelimeler: Engel Yüksekliği, Foto diyot, Organik arayüzey.

1. MATERYAL VE YÖNTEM

Tez çalışmasında; fenol kırmızısı boyar maddesi organik arayüzey olarak kullanılarak farklı üst kontaklarla organik/inorganik yarıiletken hibrit aygıtlar üretilmiştir. Şekil 1.1'de MIS hibrit yapının şematik gösterimi verilmiştir. Üretilen kontakların akım-gerilim ve kapasitans-gerilim ölçümleri oda sıcaklığında ve karanlıkta yapılmıştır.
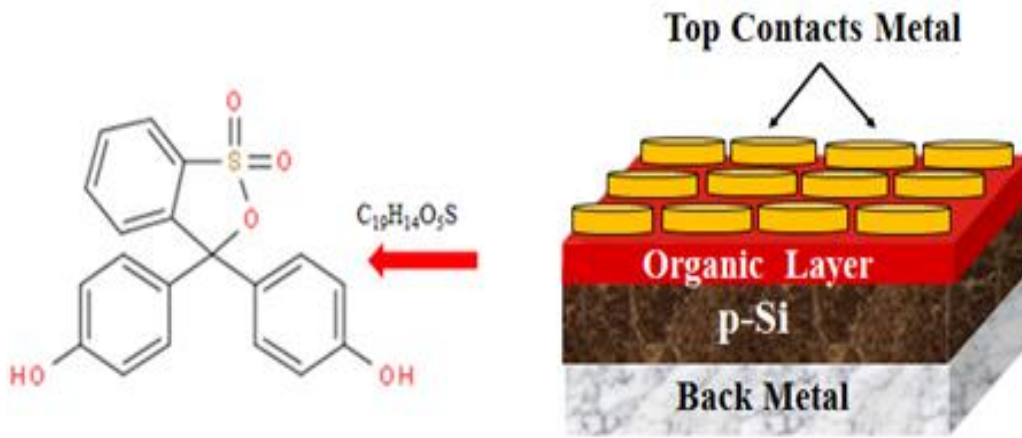
Şekil 1.1. Metal/Organik molekül/p-Si yapısının şematik gösterimi.

Aygıtın akım-voltaj ölçümlerinden elde edilen grafiklerden, hibrit yapının doğrultucu özelliği incelendi ve engel yüksekliği ve idealite faktörü gibi önemli elektriksel parametreleri belirlendi. Ek olarak, Cheung ve Norde fonksiyonları kullanılarak bu iki değer yeniden hesaplanıp sonuçların doğruluğu kontrol edildi ve diyotun seri direnci hesaplandı.

Öncelikle, organik boyar madde ara yüzey katmanın elektronik özelliklere etkisini araştırmak için elektrik parametreler hesaplandı. Akim-gerilim verileri kullanarak farklı metotlardan elde edilen bulgulara göre, ara yüzey içeren örneklerin elektriksel parametreleri daha iyi ve aygıtın performansı daha yüksektir.

Farklı metallerle oluşturulan üst kontakları doğrultucu özelliği detaylı incelendi. Metalin iş fonksiyonun aygıtın engel yüksekliğine ve diğer elektriksel parametrelere etkisi yine farklı metotlarla incelendi. Elektriksel parametrelerin iş fonksiyonu bağımlılığı özellikle organik arayüzey içermeyen numuneler için ele alindi.

2. BULGULAR VE TARTIŞMA

Bu tez kapsamında sunulan çalışmada, daha önce kullanılmamış bir organik boyar madde yardımıyla, Al/p-Si hibrit aygıtın performansının değişimi incelenmiştir. Şekil 2.1 karanlık ortamda oda sıcaklığında yapılan akım-voltaj ölçümlerinin grafikleridir. Bu grafikte ters beslem akımının zayıf bir voltaj bağımlılığı gösterdiği, doğru beslem akımın ise gerilim ile eksponansiyel olarak arttığı görülmektedir. Arayüzey içeren ve içermeyen her iki örnek de doğrultucu özellik göstermiştir. Doğrultma oranı arayüzey içeren örnekte daha yüksektir. İdealite faktörü (n) ve engel yüksekliği (Φ_b) M/p-Si ve M/PSP/p-Si örnek için sırasıyla çizelge de verilmiştir.

Hibrit yapıda aygıtlar arayüzeylerinden kaynaklanan ideal olmayan davranışlar gösterir. Sonuç olarak, elde edilen sonuçlar engel yüksekliğinin PSP organik boyar ince film arayüzey tabakası tarafından değiştirilirbilirliğini, ve modifikasyonun olabilirliğini ortaya koymuştur.
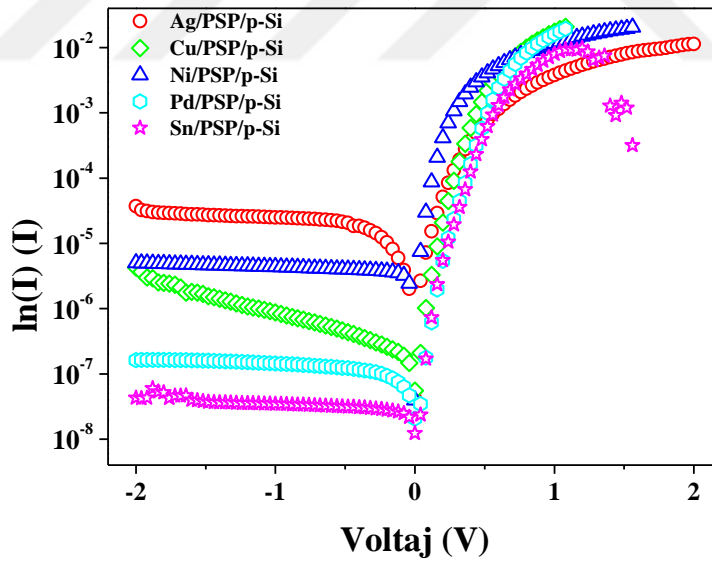

Şekil 2.1. M/PSP/p-Si aygıtlarının yarılogaritmik I-V grafikleri.

Şekil 2.1. farklı üst kontaklarla üretilen heteroeklem aygıtın I-V karakteristiğini göstermektedir. Şekilde, iş fonksiyonu farklı olan metaller için farklı karakteristikler

elde edilmiştir. En yüksek engel yüksekliği Sn metal ile edilmiştir. Hesaplamalardan elde edilen sonuçlar tabloda verilmiştir.

Table 2.1. Farklı üst kontaklar üretilen aygıtların elektrikse parametreleri

Metal	Φ_m (eV)	PSP	R	n	Φ_b (eV)	Ref	n	Φ_b (eV)
Ag	0.00		305.79	1.833	0.606		1.961	0.562
Cu	0.00		4870.16	1.146	0.687		1.289	0.558
Ni	0.00		3966	1.108	0.600		5.459	0.555
Pd	0.00		124818.8	1.272	0.724		2.802	0.648
Sn	0.00		7406.6	1.054	0.738		2.518	0.707
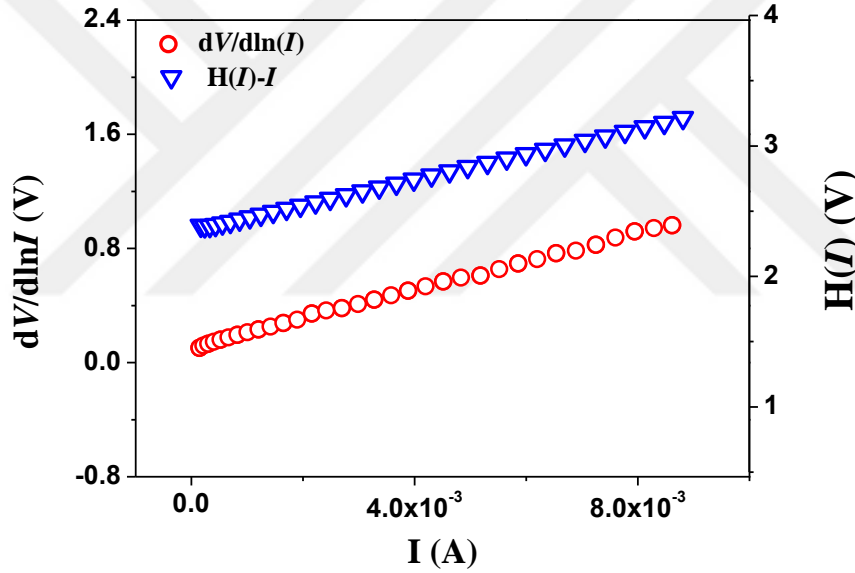
Şekil 2.2. Ag/PSP/p-Si hibrit aygıtın dV/dlnI-I ve H(I)-I grafikleri.

Şekil 3.2. Ag/PSP/p-Si hibrit aygıtın dV/dlnI-I ve H(I)-I, Cheung fonsiyonları grafikleridir. Grafiğin eğimi direnci, kesim noktası da idealite değerin verir. H(I)-I grafiğinin eğimi seri direnci kesim noktası da engel yüksekliğini verir. En yüksek engel yüksekliği düşük iş fonksiyonuna sahip olan Sn metal ile elde edilmiştir. Ayrına Sn üst kontaklı organik bileşenli aygıtın engel yüksekliği de referans numuneden büyüktür. Bu sonuçlar aygıtın elektrik özelliklerini metal iş fonksiyonuna ve arayüzeye bağımlılığını doğrulanmıştır.
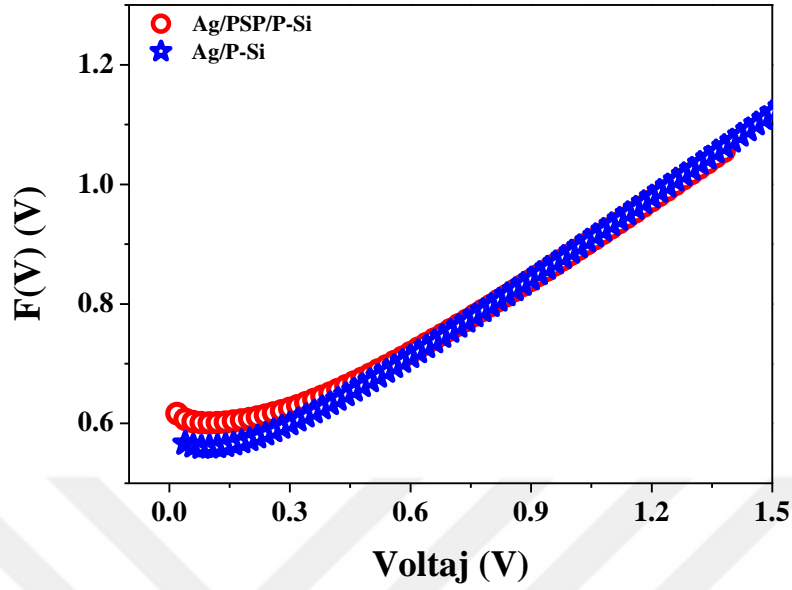
Şekil 2.3. Ag/p-Si ve Ag/PSP/p-Si hibrit aygıtın F(V)-V grafikleri.

Şekil 2.3. Ag/p-Si ve Ag/PSP/p-Si hibrit aygıtın F(V)-V grafiklerini göstermektedir. Bu grafikler yardımıyla seri direnç ve engel yüksekliği değerleri hesaplanmıştır. Bu metottan elde edilen engel yüksekliği değerleri diğer iki metottan elde edilen değerlerle uyumlu çıkmıştır. Burada yine arayüzey içeren örnekler daha büyük engel yüksekliği değerine sahiptir. Arayüzeyin olumlu etkisi bu metotla da doğrulanmıştır. Seri direnç değerleri yüksektir, bunun sebebi metodun kendi doğasından kaynaklanmaktadır ve bu sonuç litaraturle uyumludur.

Ag/PSP/p-Si hibrit aygıtın farklı frekanslar altında alınan C-V grafikleri Şekil 2.4.'te gösterilmektedir. Ters beslem durumunda kapasitans neredeyse sabit iken, düz beslemde kapasitans değeri voltaj bağımlı olarak artmıştır. Ayrıca, frekans değeri yükseldikçe kapasitans değeri düşmüştür. Bunun nedeni, arayüzey yüklerinin yüksek frekanslarda A.C sinyali takip edemesidir. Ayrıca, ara yüzey içeren numunelerin kapasitansı referans numuneden farklı capasitiv etki göstermiştir. Elde edilen bu sonuçlar literatürle uyumludur.
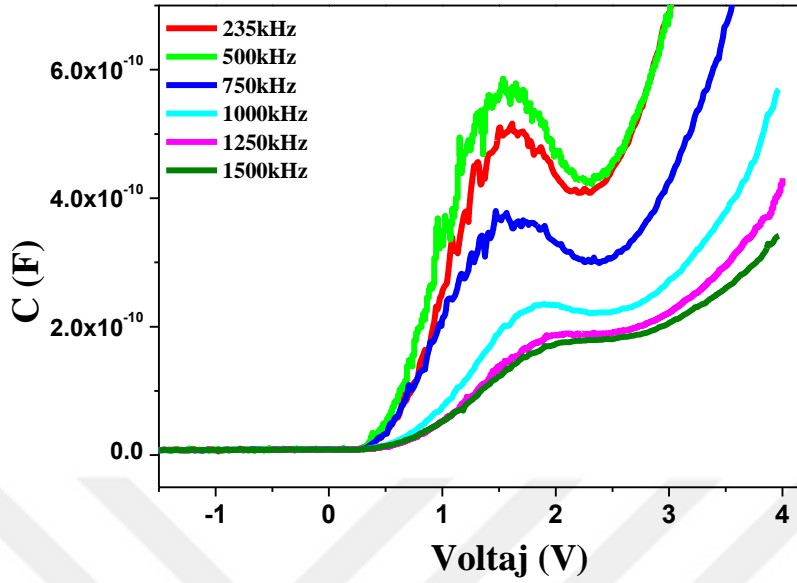
Şekil 2.4. Ag/PSP/p-Si hibrit aygıtın farklı frekanslar altında alınan C-V grafikleri.

Bu araştırmanın özgün değeri ve bilimsel açıdan önemi aşağıdaki şekilde vurgulanabilir:

(i) Bu çalışmada, hedeflenen PSP organik arayüzey kullanılarak doğrultucu kontak üretilebilirliği, ve kontak karakteristiklerinin organik materyal yardımıyla modifiye edilebilirliği, yarı iletken aygıt üretimi açısından çok büyük öneme sahiptir. Bununla beraber, birden fazla sayıda sistematik olarak üretilip, incelenen organik/inorganik yarıiletken eklemlerin akım-voltaj ölçümleri beklentiler doğrultusunda sonuçlanmış ve elektronik aygıt üretimine elverişliliği rapor edilmiştir.

(ii) Bu çalışmanın birincil önemi seçilen organik boyar maddenin elektronik aygıt performansını iyileştirmesine ilişkindir. Organik boyar maddenin (fenol kırmızısı) Schottky tipi kontaklarda arayüzey elemanı materyali olarak kullanıp, bu kontakların doğrultucu ya da omik özelliklerini incelemesi ve akım-voltaj (I-V) ve kapasitans-voltaj/frekans (C-V/C-F) ölçümleri ve grafikler yardımıyla doğrultucu özellik gösterdiği ortaya koyulmuştur. Daha önce arayüzey elemanı olarak kullanılmamış olan bu organik boyar madde ile elektronik özelliklerin iyileştiği organik arayüzey içermeyen referans aygıt ile karşılaştırmalı olarak gösterilmiştir.

(iii) Bu çalışmanın ikincil önemi seçilen organik molekül ile doğrultucu elde edildikten sonra, farklı üst kontaklar ile üretilen aygıtların özelliklerine ilişkindir. Elde edilen bulgular yardımıyla, organik arayüzey filmin farklı üst kontaklar yine doğrultucu özellik gösterdiği, yine Schottky diyot fabrikasyonu için iyi bir aday olduğu ortaya konmuştur.

3. SONUÇ

Fenol kırmızısı boyar maddesinin bir elektronik aygıtın metal yarıiletken arayüzeyinde ilk defa kullanılması tezin temel özgünlüğünü oluşturmaktadır. Bu çalışmada elde edilen bulgular fenol kırmızısı organik boyar maddesinin üretilen hibrit aygıtın elektriksel parametrelerini iyileştirdiğini ve bu parametrelerin organik arayüzey ile modifiye edilebilirliğini göstermiştir. Ayrıca, ışık altında yapılan ölçümler sayesinde aygıtın düşük beslem değerlerinde duyarlılığa sahip olduğu görülmüştür. Ek olarak, aygıtın ışık duyarlılığını ve optoelektronik uygulamalarının olasılığını araştırmak için yapılan analizlerde, kullanılan aygıtın yeterince ışık duyarlılığına sahip olduğu ve optoelektronik teknolojisinde fotodiyot yapımında kullanılabileceği rapor edilmiştir.

CURRICULUM VITAE

Sabiha Abdullah OMARBLI was born in 1978, in Dyala province, Iraq. She completed primary, secondary and high school in Erbil district. She graduated from Physics Department in Education college in Salahaddin University in 2000. She started her MSc. program in the department of Physics in Institute of Science of Van Yuzuncu Yil University in Van -Turkey, on September 2017.

Date: 22/01/2020

Thesis Title: **"The Investigation of The Effect of Metal Type on The Electrical Properties of Hybrid Structure Based on Functional Dye"** The title of the mentioned thesis, above having total 81 pages with cover page, introduction, main parts and conclusion, has been checked for originality by Turnitin computer program on the date of 22.01.2020 and its detected similar rate was 15 % according to the following specified filtering

Originality report rules:

- Excluding the Cover page,
- Excluding the Thanks,
- Excluding the Contents,
- Excluding the Symbols and Abbreviations,
- Excluding the Materials and Methods
- Excluding the Bibliography,
- Excluding the Citations,
- Excluding the publications obtained from the thesis,
- Excluding the text parts less than 7 words (Limit match size to 7 words)

I read the Thesis Originality Report Guidelines of Yuzuncu Yil University for Obtaining and Using Similarity Rate for the thesis, and I declare the accuracy of the information I have given above and my thesis does not contain any plagiarism; otherwise I accept legal responsibility for any dispute arising in situations which are likely to be detected.

Sincerely yours,

22.01.2020
Date and signature

Name and Surname: Sabiha Abdullah OMARBLI

Student ID#: 17900002006

Science: Physic

Program: Solid State Physics

Statute: M. Sc. X   Ph.D. ☐

APPROVAL OF SUPERVISOR
SUITABLE

Assoc. Prof. Dr. Arife GENÇER İMER

(Title, Name-Surname, Signature)

APPROVAL OF THE INSTITUTE
SUITABLE

(Title, Name-Surname, Signature)

Prof.Dr.Suat ŞENSOY
Enstitü Müdürü